The Surface Modification of Zeolite Y in Composite Selective
Layer of Hollow Fiber Membrane for Separation of $CO_2/CH_4$
mixture

Mr. Thakorn Wichaidit

A  Thesis Submitted in Partial Fulfillment of the Requirements
for the Degree of Master of Engineering in Chemical Engineering
Department of Chemical Engineering
Faculty of Engineering
Chulalongkorn University
Academic Year 2018
Copyright of Chulalongkorn University

การปรับปรุงพื้นผิวซีโอไลต์วายในชั้นเลือกผ่านคอมพอสิตชนิดเส้นใยกลวงสำหรับการแยกแก๊ส
ผสมของคาร์บอนไดออกไซด์/มีเทน

นายธกร วิชัยดิษฐ

วิทยานิพนธ์นี้เป็นส่วนหนึ่งของการศึกษาตามหลักสูตรปริญญาวิศวกรรมศาสตรมหาบัณฑิต
สาขาวิชาวิศวกรรมเคมี ภาควิชาวิศวกรรมเคมี
คณะวิศวกรรมศาสตร์ จุฬาลงกรณ์มหาวิทยาลัย
ปีการศึกษา 2561

Thesis Title          The Surface Modification of Zeolite Y in Composite
                      Selective Layer of Hollow Fiber Membrane for
                      Separation of $CO_2/CH_4$ mixture
By                    Mr. Thakorn Wichaidit
Field of Study        Chemical Engineering
Thesis Advisor        Dr. Chalida  Klaysom
Thesis Co Advisor     Dr. Kajornsak Faungnawakij

        Accepted by the Faculty of Engineering, Chulalongkorn University in Partial
Fulfillment of the Requirement for the Master of Engineering

                                          Dean of the Faculty of Engineering
          (Professor Dr. SUPOT TEACHAVORASINSKUN)

THESIS COMMITTEE
                                          Chairman
          (Associate Professor Dr. Varong Pavarajarn)
                                          Thesis Advisor
          (Dr. Chalida  Klaysom)
                                          Thesis Co-Advisor
          (Dr. Kajornsak Faungnawakij)
                                          Examiner
          (Dr. Pongtorn Charoensuppanimit)
                                          External Examiner
          (Associate Professor Dr. Chirakarn Muangnapoh)

จุฬาลงกรณ์มหาวิทยาลัย
CHULALONGKORN UNIVERSITY

ธกร วิชัยดิษฐ : การปรับปรุงพื้นผิวซีโอไลต์วายในชั้นเลือกผ่านคอมพอสิตชนิดเส้นใยกลวงสำหรับการแยกแก๊ส
ผสมของคาร์บอนไดออกไซด์/มีเทน. ( The Surface Modification of Zeolite Y in
Composite Selective Layer of Hollow Fiber Membrane for Separation of
$CO_2/CH_4$ mixture) อ.ที่ปรึกษาหลัก : ดร.ชลิดา คล้ายโสม, อ.ที่ปรึกษาร่วม : ดร.ขจรศักดิ์ เฟื่องนวกิจ

งานวิจัยนี้มุ่งเน้นผลิตและทดสอบเยื่อเลือกผ่านมิกซ์เมทริกซ์ชนิดเส้นใยกลวงสำหรับใช้ในการแยกก๊าซ
คาร์บอนไดออกไซด์/มีเทน โดยศึกษาผลของการปรับปรุงพื้นผิวซีโอไลต์วายเพื่อปรับปรุงความเข้ากันของสารเติมแต่งกับพอลิ
เมอร์เมทริกซ์และการกระจายตัวของสารเติมแต่งต่อคุณสมบัติของเยื่อเลือกผ่านและสมรรถนะการแยกก๊าซ โพลิซันโฟนถูก
นำมาใช้เป็นชั้นรองรับซึ่งถูกเคลือบด้วยชั้นเลือกผ่านที่ทำจากโพลีอีเทอร์บลือกเอไมด์ผสมกับซีโอไลต์วายหรือซีโอไลต์วายที่
ผ่านการปรับปรุงพื้นผิวด้วยสาร [3-(2-อะมิโนเอทิลอะมิโน)โพรพิล]ไตรเมท็อกซี่ไซเลน ผลการทดลองพบว่าอนุภาคสารเติม
แต่งเริ่มเกาะกลุ่มกันเมื่อเติมที่ 10 เปอร์เซ็นต์โดยมวล และ 15 เปอร์เซ็นต์โดยมวลสำหรับเยื่อเลือกผ่านที่มีการเติมซีโอไลต์
วายและเยื่อเลือกผ่านที่มีการเติมซีโอไลต์วายที่ผ่านการปรับปรุงพื้นผิวตามลำดับ อย่างไรก็ตามกลุ่มของอนุภาคสารเติมแต่งยัง
สามารถกระจายตัวที่ดีอยู่และไม่ปรากฏช่องว่างระหว่างอนุภาคกับเนื้อโพลิเมอร์ การเพิ่มสารเติมแต่งจาก 0 เป็น 15
เปอร์เซ็นต์โดยมวลช่วยเพิ่มสมรรถนะการแยกก๊าซของเยื่อเลือกผ่านได้เพราะว่าโครงสร้างซีโอไลต์วายช่วยเพิ่มการซึมผ่านของ
ก๊าซคาร์บอนไดออกไซด์มากกว่าก๊าซมีเทน แต่สมรรถนะการแยกก๊าซของเยื่อเลือกผ่านลดลงเมื่อทำการเพิ่มปริมาณอนุภาคจาก
10 เป็น 20 เปอร์เซ็นต์โดยมวล เนื่องจากโพลิเมอร์มีความแข็งมากขึ้นและการเกาะกลุ่มของอนุภาคทำให้เกิดบริเวณที่ไม่มีการ
เลือกผ่าน โดยพบเงื่อนไขการเติมอนุภาคที่ดีที่สุดที่ 5 เปอร์เซ็นต์โดยมวลสำหรับอนุภาคทั้งสองประเภท โดยที่เยื่อเลือกผ่านที่มี
การเติมซีโอไลต์วายสามารถปรับปรุงความสามารถในการซึมผ่านก๊าซคาร์บอน ไดออกไซด์และค่าการเลือกผ่านก๊าซคาร์บอน
ไดออกไซด์/ก๊าซมีเทนจาก 27.48 เป็น 45.06 บาร์เรอร์ และ 10.97 เป็น 19.82 ตามลำดับ ในทำนอง
เดียวกันเยื่อเลือกผ่านที่มีการเติมซีโอไลต์วายที่ผ่านการปรับปรุงพื้นผิวสามารถปรับปรุงความสามารถในการซึมผ่านก๊าซ
คาร์บอนไดออกไซด์และค่าการเลือกผ่านก๊าซคาร์บอนไดออกไซด์/ก๊าซมีเทนจาก 27.48 เป็น 51.72 บาร์เรอร์ และ
10.97 เป็น 19.82 ตามลำดับ โดยพบว่าการดำเนินการที่ 2 บาร์ และ 30 องศาเซลเซียสเป็นสภาวะดำเนินการที่เหมาะสม
ที่สุด และที่ปริมาณการเติมอนุภาคเดียวกัน เยื่อเลือกผ่านที่มีการเติมซีโอไลต์วายที่ผ่านการปรับปรุงพื้นผิวให้การกระจายตัว และ
สมรรถนะการแยกก๊าซที่ดีกว่าตัวที่เติมซีโอไลต์วายที่ไม่มีการปรับคุณสมบัติพื้นผิว

จุฬาลงกรณ์มหาวิทยาลัย
CHULALONGKORN UNIVERSITY

| | | |
|---|---|---|
| สาขาวิชา | วิศวกรรมเคมี | ลายมือชื่อนิสิต ................................................ |
| ปีการศึกษา | 2561 | ลายมือชื่อ อ.ที่ปรึกษาหลัก ............................. |
| | | ลายมือชื่อ อ.ที่ปรึกษาร่วม ............................. |

# # 5970437321 : MAJOR CHEMICAL ENGINEERING

Thakorn Wichaidit : The Surface Modification of Zeolite Y in Composite Selective Layer of Hollow Fiber Membrane for Separation of $CO_2/CH_4$ mixture. Advisor: Dr. Chalida Klaysom Co-advisor: Dr. Kajornsak Faungnawakij

This work focused on the fabrication and evaluation of composing hollow fiber mixed matrix membranes (MMMs) incorporated by zeolite Y for $CO_2/CH_4$ separation. The effects of surface modification of zeolite Y to improve compatibility of filler and polymer dispersibility of the filler in the polymer matrix on properties and separation performance of the membrane were investigated. A polysulfone (PSF) was used as a support hollow fiber and a selective layer composing of polyether-block-amide (Pebax) and zeolite Y (ZeY) and surface modification of zeolite Y (mo-ZeY) was coated on support. A [3-(2-Aminoethylamino)propyl]trimethoxysilane (AEAPTMS) was used to grafted on surface of pristine zeolite Y. The effects of filler loading at 0-20 wt% on membrane property and separation performance were investigated. The results revealed that the filler started to agglomerate at 10 wt% for ZeY and at 15 wt% for mo-ZeY. However, the aggregated filler cluster still showed fairly good dispersion. In addition, the interfacial gap and void between the disperse phase and the continuous phase of MMMs did not appeared. The addition of ZeY and mo-ZeY from 0 wt% to 5 wt% provided a positive impact on membrane performance because $CO_2$ can diffuse through the filler pores easier than $CH_4$. The decrease in membrane performance was obtained with increasing filler content from 10 wt% to 20 wt% due to polymer rigidified and filler agglomeration that from nonselective path. The optimal condition of filler loading was found to be 5 wt% for both filler. The 5 wt% ZeY/Pebax membrane can improve $CO_2$ permeability and $CO_2/CH_4$ selectivity from 27.48 to 45.06 barrers and 10.97 to 19.82, respectively. In the same ways, the 5 wt% mo-ZeY/Pebax membrane can improve $CO_2$ permeability and $CO_2/CH_4$ selectivity from 27.48 to 51.72 barrers and 10.97 to 21.53, respectively. The optimal operating conditions were found at 2 bars and 30°C due to it provides highest separation performance. The result showed that at the same filler loading, the mo-ZeY/Pebax provide a better dispersibility and separation performance compared to ZeY/membrane.

| Field of Study: | Chemical Engineering | Student's Signature |
| --- | --- | --- |
| | | ............................. |
| Academic Year: | 2018 | Advisor's Signature |
| | | ............................. |
| | | Co-advisor's Signature |
| | | ......................... |

# ACKNOWLEDGEMENTS

Thakorn Wichaidit

# TABLE OF CONTENTS

**Page**

# LIST OF TABLES

จุฬาลงกรณ์มหาวิทยาลัย
CHULALONGKORN UNIVERSITY

# LIST OF FIGURES

**Page**

# CHAPTER 1

# INTRODUCTION

## 1.1 Motivation

Biogas has been considered as an alternative renewable energy from several organic waste sources such as agriculture, industries, and landfills. Typically, biogas consists of methane ($CH_4$, 50-70%), carbon dioxide ($CO_2$, 30-50%), and small amount of water and hydrogen sulfide [1]. Before the use of biogas, inert and corrosive gases such as $H_2S$ and water must be eliminated. There are several separation and purification approaches in carbon dioxide removal such as cryogenic distillation, absorption, adsorption, and membrane gas separation. One of proficient technologies for biogas upgrading is membrane gas separation. The advantages of membrane gas separation are low energy consumption, simplicity in operation, low operating costs, small space for installation, no requirement for chemical additives, and easy for scale-up (higher flexibility) [2]. Membranes used in biogas upgrading are mostly made of polymer because fabrication of polymeric membranes are easy and low cost than inorganic membrane.

For gas mixture separations, the polymeric membranes are mostly applied. Polymeric membranes can be divided into two kind, glassy and rubbery polymeric membranes. Glassy membranes can provide the low $CO_2$ permeability but high $CO_2/CH_4$ selectivity due to rigid polymer structure. On the other hand, glassy membranes can give the high $CO_2$ permeability but low $CO_2/CH_4$ selectivity because of flexible polymer structure. Polyether block amide (Pebax 1657) is a copolymer consists of polyamide (PA) that has rigid section structure and Polyethylene oxide (PEO) that has soft structure with ratio 40 and 60 weight ratio, respectively. Pebax has high mechanical and thermal stability. It can be provided good $CO_2/CH_4$ separation performance. Because of these properties, Pebax are preferable compared to other material. In addition, we can further improve gas separation performance of polymeric membranes by incorporating inorganic filler such as zeolite, carbon molecular sieve (CMS), silica particle, metal oxide, carbon nanotube (CNT), metal

organic framework (MOF), and graphene into polymer matrix to combine the advantages of an organic polymer with inorganic fillers would improve the gas separation performance. Among the organic fillers, zeolite is wildly selected because their molecular sieve properties such as specific pore diameters that no steric hindrance for gas molecule like carbon dioxide, methane, and nitrogen to enter the pore and give higher $CO_2$ permeance than other inorganic fillers. The zeolite has potential to accomplish the gas separation performance of polymeric membrane while keeping their advantage **[3-6]**. However, the main problem in incorporating inorganic filler into polymer matrix is "interfacial void" between polymer matrix and filler due to poor interaction of zeolite external surface and polymer matrix. This problem results in the decline of membrane selectivity. If we want to overcome this interfacial defect, we need to improve the interaction between the two phases. So, in this study, the modification of zeolite surface for improving interaction between polymer and zeolite for a better biogas upgrading performance will be investigated.

## 1.2 Objective

This work focused on the fabrication, characterization, and evaluation of composite hollow fiber mixed matrix membranes (MMMs) incorporated by zeolite for $CO_2/CH_4$ separation. The effects of surface modification of zeolite Y-type to improve compatibility of filler and polymer dispersibility of the filler in the polymer matrix, and separation performance of the membrane were investigated.

## 1.3 Scope of work

Composite hollow fiber mixed matrix membranes consisting of a support layer and a selective layer were fabricated. The effects of modified and unmodified surface filler in selective layer as well as its loading percentage on membranes properties and gas separation performance were investigated.

1.3.1 Surface modification of zeolite was carried out by a grafting method with an di-aminosilane coupling agent under the fixed parameters as follows:

- Unmodified filler: Zeolite Y-type (FAU frame work type) with 15 Si/Al mole ratio

- Aminosilane coupling agent:      [3-(2-Aminoethylamino)propyl]tri methoxysilane (AEAPTES)
- Polar medium solvent:      Ethyl alcohol (EtOH)
- Ratio of zeolite/ silane/ solvent:      2 gram of zeolite/ 8 mL of AEAPTMS/ 100 mL of ethyl alcohol (EtOH)
- Reaction temperature:      85 °C
- Reaction time:      24 hours

1.3.2 The support layer of composite hollow fiber mixed matrix membranes (MMMs) was fabricated by a phase inversion method under the following conditions:

- Dope solution:      20 wt% of Polysulfone (PSF) in solvent N-Methyl-2-Pyrrolidone (NMP)
- Bore fluid:      Reverse Osmosis (RO) water
- Air gap of support fabrication:      10 cm
- Mass flow rate of dope solution:      1.2 g/min
- Mass flow rate of bore fluid:      0.98 g/min

1.3.3 The selective layer was coated on the hollow fiber support by a dip-coating method under the following parameters:

- Polymer solution:      5 wt% of Polyether-block-amide (Pebax) in solvent mixture between 70 wt% of EtOH and 30 wt% of RO water
- Filler type:      Zeolite Y and surface modified zeolite Y
- Filler loading:      0 - 20 wt%

1.3.4 The gas separation performance was tested in gas permeation apparatus at a steady state and an isothermal condition under the following conditions:

- In let stream:      Mixed gas of $CO_2/CH_4$ (50:50 mole ratio) at 20 mL/min
- Carrier gas:      Helium at 45 mL/min
- pressure:      2-6 bar

- Temperature:                      30-70 $^{\circ}$C

     1.3.5 Membrane and material properties were characterized by.

- Filler surface area and pore volume:    Brunauer-Emmett-Teller (BET)
- Crystal structure of filler and MMMs:    X-Ray Diffraction (XRD) method
- Functional groups on surface filler:     Fourier transform infrared spectroscopy – attenuated total reflectance (FTIR–ATR)
- Morphology of filler and MMMs:      Scanning electron microscope (SEM)
- Glass transition temperature:         Differential scanning calorimetry (DSC)

จุฬาลงกรณ์มหาวิทยาลัย

CHULALONGKORN UNIVERSITY

# CHAPTER 2

# BACKGROUND AND LITERATURE REVIEW

## 2.1 Background about biogas

Biogas is a combustible gas, generated by a decomposition of organic compounds via an anaerobic digestion process. The organic matter is fermented with bacteria communities for generating biogas with three steps of fermentation as follows [7]:

I. Firstly, the digestion process is taken place via a hydrolysis reaction that can break down insoluble organic polymers (carbohydrates, protein, and fat) into small soluble molecules, such as sugar, amino acid, fatty acid.

II. Secondly, the acidogenic bacteria converts sugars, amino acid, and fatty acids into volatile organic acids such as acetic acid, propionic acid, and butyric acid. Moreover, the acidogenic bacteria also further converts the volatile organic acids into hydrogen, ammonia, and carbon dioxide.

III. Finally, the methanogens an archaea bacteria in anoxic environment converts the product from step II into methane and carbon dioxide which are the major components of biogas.

Biogas is thus a renowned and environmental friendly energy resource, consisting of three main components.

(1) Methane ($CH_4$) 55-70% v/v

(2) Carbon dioxide ($CO_2$) 30-45% v/v

(3) Small amount of hydrogen sulfide ($H_2S$) and water ($H_2O$)

If $CO_2$ and other impurities are removed from raw biogas, the obtained biomethane can be fed to natural gas line and can be compressed to use as compressed natural gas (CNG). Generally, biogas purification processes consist of two major steps, namely pretreatment and biogas upgrading as shown in **Figure 1**
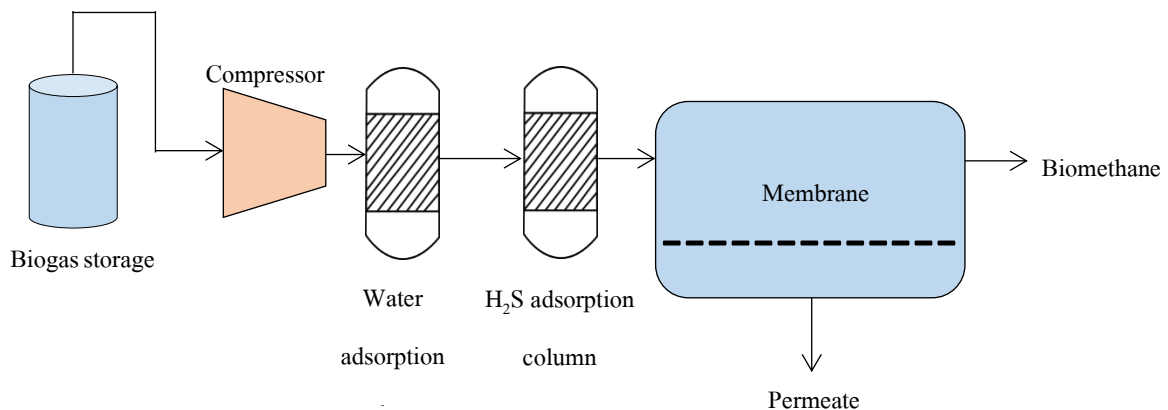
**Figure 1** Biogas purification process diagram

I. Biogas in a storage tank is compressed by a compressor and fed to the dehydration unit for water removal.

II. The dehydration process is normally carried out by an adsorption column with silica or alumina as the adsorber.

III. After the dehydration process, the dry gas was compressed and sent to the hydrogen sulfide removal process usually by an adsorption column with carbon molecular sieve (CMS) as the adsorber.

IV. Lastly, the biogas without corrosion gas was compressed to biogas upgrading process by gas membrane separation process.

## 2.2 Background on membrane separation process

### 2.1.1 Molecule transport theory in membrane

One type of gas is separated from a feed gas mixture via a selective barrier of membrane based on the principle that some gases can transport through the membrane faster than others. For gas separation membrane, especially $CO_2/CH_4$ gas separation, the separation of gas molecules follows the so-called solution-diffusion mechanism. Considering solution-diffusion model, the selectivity is controlled by molecular structure of polymer that permits specific gas molecules to pass through membranes based on their solubility and diffusion of gas [8]. The gas permeation through a dense membrane is depicted in **Figure 2**. This mechanism consists of three steps as follows [9-11]:

1) Absorption: The feed gas is absorbed into the membrane

2) Diffusion: The gas diffuses through the selective barrier due to a driving force called the concentration gradients.

3) Desorption: The gas is released from the surface of the membrane into the permeate side.
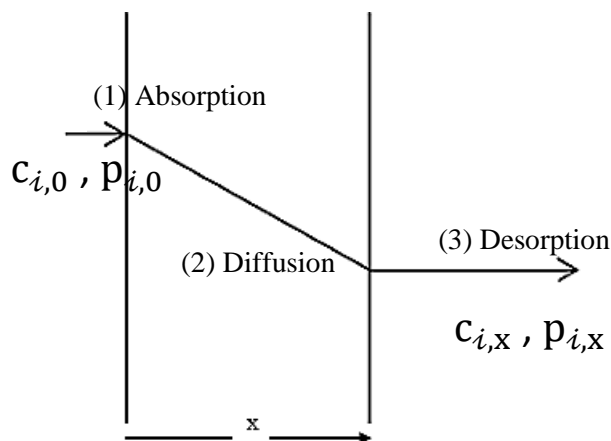


**Figure 2** Gas permeation through the dense membrane

The flux of gas through the membrane is explained by Fick's law **(Eq2.1)**.

$$J_i = -D_i \frac{dc_i}{dx} \qquad \textbf{Eq2.1}$$

Where $J_i$ = flux of component $i$

$D_i$ = diffusion coefficient of component $i$ in membrane

$c_i$ = concentration of component $i$

$x$ = membrane thickness

By integrating **Eq2.1** with the boundary condition of membrane thickness from 0 to x and the component $i$ concentration from $c_{i,0}$ to $c_{i,x}$ , the flux can be expressed in **Eq2.2**

$$J_i = D_i \frac{(c_{i,0} - c_{i,x})}{x} \qquad \textbf{Eq2.2}$$

The solubility coefficient or the sorption coefficient of component $i$ in membranes is a ratio of the gas concentration to the partial pressure of gas and can be rearranged into **Eq2.3**

$$c_i = S_i p_i \qquad \textbf{Eq2.3}$$

Where $S_i$ = solubility coefficient between component $i$ and membrane

$c_i$ = concentration of component $i$

$p_i$ = partial pressure of component $i$

By substituting **Eq2.3** into **Eq2.2**, the gas flux of one-dimensional steady-state through the membrane can be defined as follows:

$$J_i = D_i S_i \frac{(p_{i,0} - p_{i,x})}{x} \qquad \textbf{Eq2.4}$$

The gas permeability of component $i$ can be expressed in terms of the solution and diffusion coefficient as follows:

$$\mathcal{P}_i = D_i \, S_i \qquad \textbf{Eq2.5}$$

Where $\mathcal{P}_i$ = component $i$ permeability

$D_i$ = diffusion coefficient between component $i$ and membrane

$S_i$ = solubility coefficient between component $i$ and membrane

$p_{i,0} - p_{i,x}$ = transmembrane partial pressure of component $i$

Therefore, when substituting the permeability ($\mathcal{P}_i$) from **Eq2.5** into **Eq2.4**, the gas permeability equation can be rearranged in **Eq2.6**

$$\mathcal{P}_i = \frac{J_i \, x}{(p_{i,0} - p_{i,x})} \qquad \textbf{Eq2.6}$$

Where $\mathcal{P}_i$ = component $i$ gas permeability

$J_i$ = component $i$ gas flux

$p_{i,0} - p_{i,x}$ = component $i$ transmembrane partial pressure

$x$  = membrane thickness

the permeability of $CO_2$ and $CH_4$ in gas mixture.

For the gas mixture, gas selective separation factor of membrane is defined as **Eq2.7**

$$\alpha_{ij} = \frac{(y_i \, / \, y_j)}{(x_i \, / \, x_j)}$$ **Eq2.7**

Where $\alpha_{ij}$ = component $i$ membrane selective factor

$y_i$ = component $i$ mol fraction in permeate side

$y_j$ = component $j$ mol fraction in permeate side

$x_i$ = component $i$ mol fraction in retentate side

$x_j$ = component $j$ mol fraction in retentate side

### 2.2.2 Membrane materials

Membranes for gas separation can be classified into three types based on the material used.

1) Inorganic membranes

Inorganic membranes are made of metal or ceramic. The gas flux and the permeability in inorganic membranes depend on the protonic and electronic conductivities of the material used. It can be operated in high range of temperature as 600-900°C. Generally, inorganic membranes provide superior gas separation performance with high selectivity and permeability. However, there are some limitations of inorganic membranes that is difficult for fabrication and thus expensive. Therefore, it is not commonly used for biogas upgrading **[12]**.

2) Polymeric membranes

Polymeric membranes can be sub classified into two types based on polymer types: rubbery and glassy polymer.

The rubbery polymer such as Polydimethylsiloxane (PDMS) exhibits soft and elastic structure due to segments of polymer backbone that can rotate freely around their axis. So, it can give the high permeability but low selectivity. On the other hand, glassy polymer such as polysulfone, polyetherimide obtains steric hindrance along the polymer backbone which disallows rotation of polymer segments resulting in rigid and tough structure. So, the glassy polymer can provide the membrane with low permeability but high selectivity.

3) Mixed matrix membranes

Mixed matrix membranes (MMMs) are consisted of inorganic fillers dispersing in a matrix of polymer. The selection of polymer and inorganic filler pair is of importance for the synthesis this class of membranes. MMMs are able to enhance membrane performance due to combination gas separation characteristic of filler and polymer together.

**2.2.3 Fabrication of membranes**

Generally, membrane is fabricated via a phase inversion technique. Hollow fiber membranes can be fabricated by adopting the dry-jet wet quench spinning process. **Figure 3 [13]** shows the dry-jet wet quench spinning process diagram and **Figure 4 [14]** shows the double-orifice spinneret head close-up in the dry jet/wet quench spinning process. In the spinning process, the dope solution and the bore fluid are co-extruded through the spinneret head under specific flow rates and temperature condition. The dope solution is extruded from a hot spinneret and bore fluid is extruded from the center space, generating the hollow channel of fibers. The solvent from the spinneret hollow fiber was evaporated through air gap and outer surface of the fiber will be precipitated once it reaches the water bath. Lastly, the non-solvent in quench bath will be phase exchanged with the solvent in the dope solution in the coagulation process and polymer was precipitated to form a hollow fiber membrane. After the hollow fiber membrane passing through the quench bath was collected around a take-up drum, which is equipped with a system of gears enabling spinning at specific speeds condition.
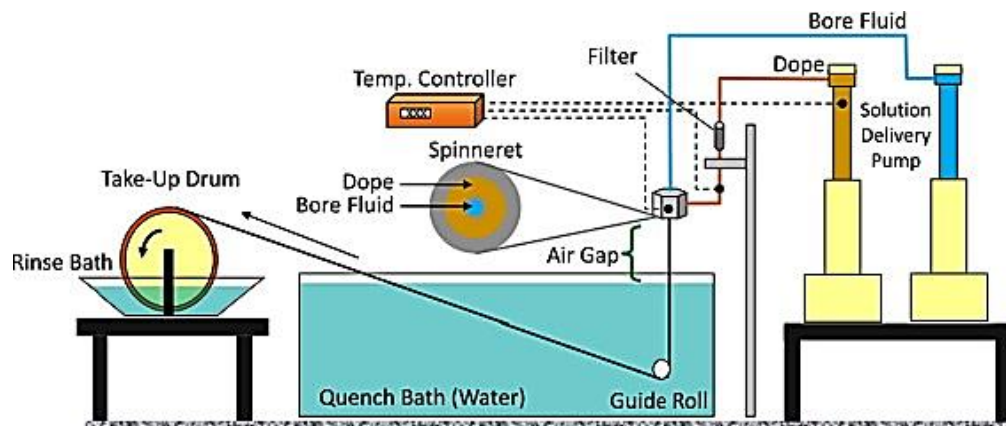
**Figure 3** The dry-jet/wet quench spinning process diagram
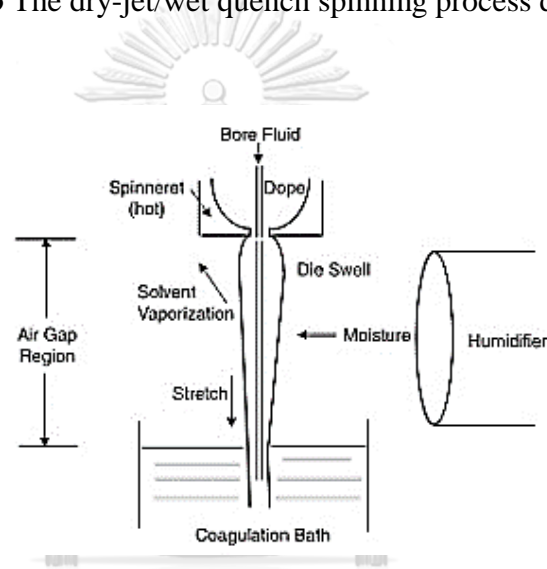


**Figure 4** The close-up of spinneret head in dry jet/wet quench spinning process

From the dry-jet/wet quench spinning process, there are many parameters that affecting to the hollow fiber membrane properties. The major effects of fabrication parameter on hollow fiber properties can be explained as follow **[15, 16]**:

1) The elongation drawing ratio

The elongation drawing ratio is a tension force from take-up drum in the dry-jet/wet quench spinning process. The effect of elongation drawing ratio on the hollow fiber membrane structure was studied by Wang et al **[16]** with polyethersulfone. It was found that macrovoids became smaller when the elongation drawing ratio was increased. In General, the macrovoids are not favorable in membrane for gas separation that normally operates at high pressure. These macrovoids can easily collapse.

2) Shear rate in the spinneret

The effect of shear rate in the spinneret was studied by Wang et al [16]. The macrovoids near the hollow fiber membrane inner surface became smaller and were eliminated when the shear rate of dope solution was increased. Air gap between spinneret and bore fluid surface

The effect of air gap between spinneret and bore fluid surface was studied by Wang et al [16]. The results found that, when increased the air gap between spinneret and bore fluid surface, gas permeation decreased because of a prolonged time for solvent evaporation.

The obtained hollow fibers from the spinneret is normally dried and undergone some post-treatment steps before being packed in a membrane module.

In general, the module of hollow fiber membranes is designed in the similar configuration as the shell and tube heat exchanger [17].
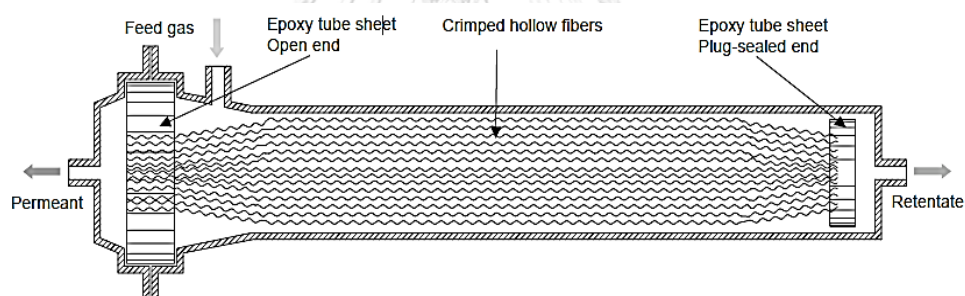


**Figure 5** The hollow fiber module

The operations for gas separation membrane can be classified into two modes [18]:

a) Inside-out mode, in which the gas mixture enters tubes side and permeates through shell side (**Figure 2.6A**).

b) Outside-in mode: in which the gas mixture enters shell side and permeates through tubes side (**Figure 2.6B**).
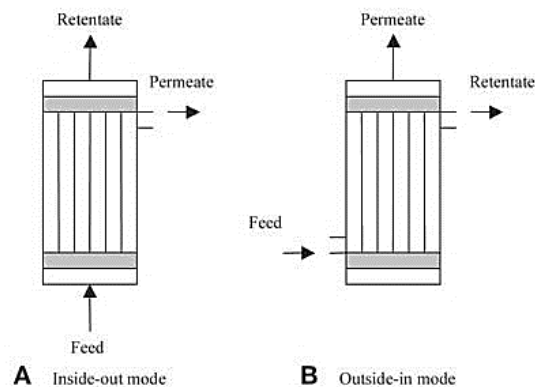
**Figure 6** Operation for gas membrane separation with hollow fiber membrane

Generally, there are several aspects to consider when designing a hollow fiber membranes and modules for the gas separation membrane **[19]**:

- Mechanical strength

A module and hollow fiber membranes must be strong enough for a long operating period. They should be able to withstand the operating pressure, operating temperature, and tolerate a corrosion from inlet chemicals.

- Hollow fiber arrangement

The hollow fiber in a module must be pack in a parallel pattern and uniformly spread in modules. Approximately 45-60% of module volume is recommended for fiber packing density.

- Economy

The cost of materials for fabricating module and hollow fiber membrane have to be considered. Moreover, the maintenance and replacement of membranes should also be token in to account.

## 2.3 Literature review

At the present, many researchers pay attention to polymeric membrane because of its low production cost, easy for fabrication, and good mechanical stability.

**Table 1** Compares $CO_2/CH_4$ separation performance from different polymeric membranes.

| Polymer | Operating condition | | | Membrane performance | | Ref. |
|---------|------|------|------|------|------|------|
| | T (°C) | P (bar) | $CO_2$:$CH_4$ (mol%) | $\mathcal{P}$ of $CO_2$ (GPU or Barrers) | $CO_2/CH_4$ selectivity | |
| Polysulfone | 25 | 3 | Single gas | 45.88 GPU | 21.25 | [20] |
| | 25 | 2 | Single gas | 12.33 GPU | 2.63 | [21] |
| | 27 | 5 | Single gas | 21.27 GPU | 19.83 | [22] |
| | 30 | 3 | 73:27 | 9.50 Barrers | 22.00 | [23] |
| | 35 | 3 | 50:50 | 9.50 Barrers | 23.80 | [24] |
| | 35 | 3 | 50:50 | 4.70 Barrers | 24.70 | [25] |
| | 35 | 4.4 | Single gas | 6.30 Barrers | 28.60 | [26] |
| | 35 | 4 | Single gas | 4.50 Barrers | 25.90 | [27] |
| | 25 | 5 | Single gas | 69.40 Barrers | 1.30 | [28] |
| Polyimide (Matrimid) | 30 | 2 | Single gas | 7.29 Barrers | 34.71 | [29] |
| | 20 | 15 | 50:50 | 11.00 GPU | 67.00 | [30] |
| | 35 | 5 | Single gas | 8.50 Barrers | 24.00 | [31] |
| | 35 | 9 | 50:50 | 4.00 Barrers | 30.00 | [32] |
| | 35 | 2 | Single gas | 8.34 Barrers | 36.3 | [33] |
| | 30 | 2 | 30:70 | 8.00 Barrers | 28.00 | [34] |
| | 25 | 10 | Single gas | 6.20 Barrers | 3.10 | [35] |
| | 35 | 10 | 50:50 | 6.20 Barrers | 28.00 | [36] |
| Polyetherimide (Ultem 1000) | 35 | 2 | Single gas | 7.60 Barrers | 35.00 | [37] |
| | | | | 1.40 Barrers | 38.00 | |
| | 25 | 15 | Single gas | 0.74 GPU | 43.10 | [38] |
| | 25 | 2 | Single gas | 148.00 GPU | 12.07 | [39] |
| Pebax 1657 | 35 | 5 | 55:45 | 10.81 GPU | 7.59 | [40] |
| | 25 | 1 | Single gas | 500.00 Barrers | 20.00 | [41] |
| | 25 | 2 | 30:70 | 500.00 Barrers | 18.00 | [42] |
| | 25 | 5 | Single gas | 55.80 Barrers | 18.00 | [43] |

From **Table 1**, Glassy polymer such as polysulfone (PSF), polyimide (PI) and polyetherimide (PEI) were largely used in many research studies and commercial application because of its high selectivity. Polysulfone is considered to be a good candidate because of $CO_2$ is preferentially adsorbed in matrix of polysulfone compare to $CH_4$ mainly due to the likeness of its structure to sulfonyl group and its higher critical temperature. Besides, polysulfone also exhibits profitable properties such as good mechanical strength, thermal resistance, chemical resistance, cost effective, and high resistance to plasticization. Polyimide and polyetherimide are preferred as it belongs to a family of high performance polymer. It possesses high glass transition temperature ($T_g$) that makes it attractive for several gas separation applications. However, polyimide and polyetherimide are low plasticization resistance at a pressure below 8 bars and highly sensitive with water vapor [20].

Rubbery polymer such as polyether-block-amide (Pebax 1657) is one of promising polymer for biogas upgrading that give high $CO_2$ permeability. Pebax is a copolymer consists of polyamide (PA) and polyethylene oxide (PEO) 0.4:0.6 weight ratio. It has good mechanical stability due to hard section structure from PA, and flexible due to soft section from PEO. Pebax is cheap and can provide good gas permeability and moderate gas selectivity for separation of $CO_2/CH_4$ mixture.

However, these polymeric membranes have two main limitations to overcome namely,

1) Trade-off between permeability and selectivity
2) Plasticization of polymeric membranes.

There are two parameters describing membrane performance; permeability and selectivity. Permeability is the ability of a specific gas to transport from one side of membrane to the other side. Selectivity is the membrane ability to separate a specific gas from mixture. These two parameters typically show inverse relationship as shown in **Figure 7** so called the trade-off graph originally proposed by Robeson [44].
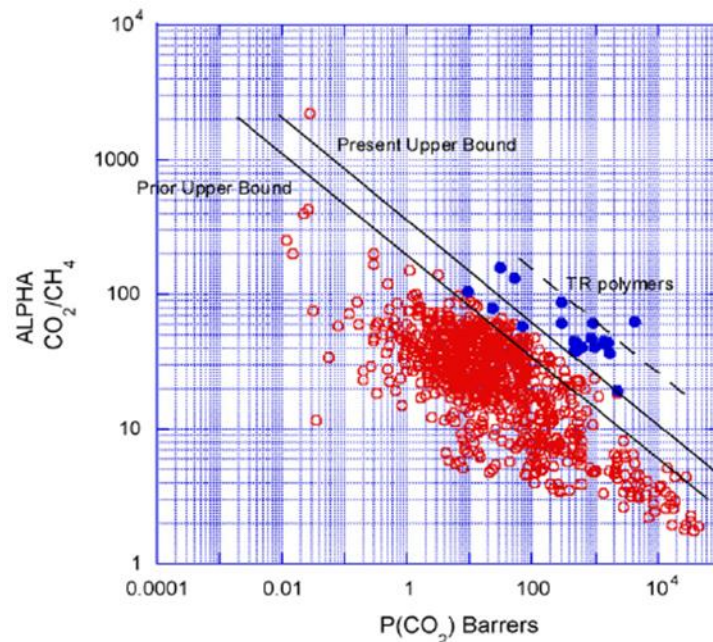
**Figure 7** Robeson's upper bound for $CO_2/CH_4$ separation

Nowadays, many researchers are focusing on the development of membrane that overcome the trade-off limits. One of the most promising strategies is by making composite materials or mix matrix membranes (MMMs). The currently developed composite membranes MMMs are discussed in detail in section **2.3.1**

Plasticization is phenomenon when plasticizing gas molecule dissolves into the polymer matrix and make polymer chains more flexible and lose the ability to separate gas. It mostly appears at a high operating pressure after a long operating time. In biogas upgrading application, polymer chain structure was interrupted and swells by the dissolved $CO_2$ molecule. The separation performance was directly affected by this phenomenon. The effect of plasticization results in an increase in $CO_2$ permeability and a drastic decrease in selectivity. The method to reduce the plasticization in polymeric membranes is by modification of polymer structure either by blending a polymer with more $CO_2$-resist polymer, thermal treatment and rearrangement of polymer, and cross-linking of polymer **[45]**.

**2.3.1 The development of MMM for $CO_2/CH_4$ separation**

One way to improve the performance of membranes for biogas upgrading is to incorporate specific microporous as filler in a polymer matrix forming mix matrix membranes (MMMs). The separation mechanism for microporous filler can be classified follows **[46]**.

1. Adsorption controlled separation by adsorptive interaction between filler framework and the molecules of permeation gas.

2. Diffusion controlled separation that depends on the relative size of the diffusing molecule of gas through pore size filler.

3. Molecular sieving that gas molecules smaller than the pores can diffuse through the filler pore.
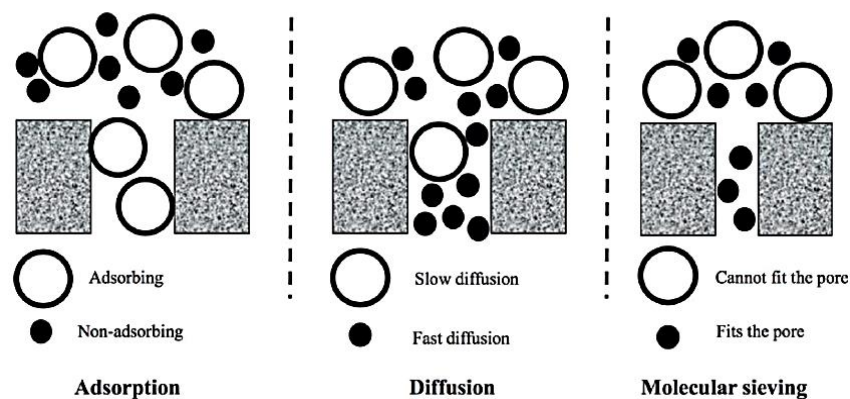


**Figure 8** A schematic shown the gas separation in microporous filler

The MMMs that incorporate with microporous filler is usually governed by a combination of these mechanisms for separation gas molecule. Zeolites are one of the most widely used molecular sieve fillers **[3-6]** for gas separation membrane. It possess uniform pore size, tetrahedral, arranged by shared oxygen at the corners of aluminosilicate geometric patterns with high thermal and chemical stability. **Table 2** compares separation performance of MMMs using different types of zeolite as the fillers.

**Table  2** Comparison for $CO_2/CH_4$ separation performance of mixed matrix membranes

| Material | | | Operating condition | | | Membrane performance | | Ref. |
|---|---|---|---|---|---|---|---|---|
| Filler | Filler loading (wt.%) | Polymer | T (°C) | P (bar) | $CO_2:CH_4$ (mol%) | $\mathcal{P}$ of $CO_2$ (Barrers) | $CO_2/CH_4$ selectivity | |
| Sapo-34 | 0 | Pebax | 25 | 4 | Single gas | 120.00 | 4.30 | [47] |
| | 30 | | | | | 138.00 | 5.30 | |
| | 0 | Pebax | 35 | 7 | Single gas | 111.00 | 17.00 | [48] |
| | 50 | | | | | 338.00 | 16.00 | |
| Zeolite Y | 0 | Polyimide | 35 | 2 | Single gas | 8.34 | 36.3 | [49] |
| | 10 | | | | | 15.02 | 39.8 | |
| | 0 | Polyimide | 35 | 2 | Single gas | 8.34 | 36.30 | [50] |
| | 15 | | | | | 9.70 | 57.10 | |
| | 0 | | | | 10:90 | 6.66 | 30.00 | |
| | 15 | | | | | 8.31 | 50.00 | |
| Zeolite X | 0 | Polyimide | 35 | 1 | Single gas | 8.34 | 1.22 | [51] |
| | 35 | | | | | 33.4 | 6.86 | |
| | 0 | Polyimide/ Polyether sulfone (20/80) | 35 | 10 | Single gas | 6.54 | 33.59 | [52] |
| | 25 | | | | | 15.04 | 38.69 | |
| Zeolite A | 0 | | | | | 6.54 | 33.59 | |
| | 25 | | | | | 5.02 | 46.05 | |
| | 0 | Polyether sulfone | 35 | 10 | Single gas | 2.80 | 32.00 | [53] |
| | 20 | | | | | 1.40 | 44.00 | |
| | 0 | Poly carbonate | 25 | 3.7 | Single gas | 8.80 | 23.60 | [54] |
| | 25 | | | | | 7.00 | 37.60 | |
| | 0 | Polyvinyl alcohol | 35 | 30 | 50:50 | 11.40 | 25.00 | [55] |
| | 50 | | | | | 11.50 | 40.60 | |

| ZSM-5 | 0 | Polyimide | 25 | 2 | Single gas | 7.29 | 34.71 | [29] |
| | 10 | | | | | 8.27 | 67.19 | |
| | 0 | Poly etherimide | 35 | 2 | Single gas | 1.40 | 38.00 | [37] |
| | 30 | | | | | 2.00 | 45.00 | |
| | 0 | Polyimide | | | | 7.60 | 35.00 | |
| | 35 | | | | | 31.00 | 39.00 | |

From **Table 2**, Sapo-34 and zeolite A can improve the $CO_2$ permeability. The $CO_2/CH_4$ selectivity increased due to the molecular sieve characteristic of Sapo-34 and zeolite A can restrict the movement of gas with similar size of pore size (3.8 Å) like $CH_4$. However, Sapo-34 and zeolite A can also decrease $CO_2$ permeability of membranes if their pores are blocked by the polymer **[53, 54]**. The decrease in $CO_2/CH_4$ selectivity was also observed when interfacial void between polymer and filler was created **[48]**.

MFI framework type (ZSM-5) can improve the membrane performance even though it was not as good as the FAU framework type (zeolite X and Y). This was because the smaller window size and less electrostatic quadrupole interaction **[56]**.

**Table 2** shows that the FAU framework type (zeolite X and Y) is considered to be a good candidate as a filler for MMMs in biogas upgrading, because the window size of FAU has no steric hindrance for gas molecule, like $CO_2$, $CH_4$, and $N_2$ to enter the pore. Comparing two FAU framework type (Y type and X type), the Si/Al ratio of zeolite Y-type ($\geq 1.5$) is larger than that in X-type ($< 1.5$). This means that the zeolite Y has lower $AlO_4^{5-}$ content and thus lower negative charge lower in zeolite Y-type. Thus, number of cations in zeolite Y-type is lower than that in X-type. Therefore, the reduction of number of micropores, micropores volume, and $CO_2$ interaction with cations in zeolite Y-type particles would be less than X-type **[57-59]**. Hence, zeolite Y can be suitable for $CO_2$ permeation because of its large pore size to facilitates the diffusion of $CO_2$. Therefore, $CO_2$ is preferential interaction with the aluminosilicate framework and the extra framework cations which leads to a favorable combination of

sorption and mobility. Once $CO_2$ is preferentially adsorbed on the zeolite pores, it blocks and restricts the transport of $CH_4$ **[60]**.

FAU framework type contains $AlO_4^{5-}$ and $SiO_4^{4-}$ tetrahedral linked to each other by oxygen atom sharing. Isomorphic substitution of Al atom with Si atom in framework causes a negative charge to be induced by $AlO_4^{5-}$ tetrahedral. To maintain the electro neutrality of zeolite, it needs the presence of cations such as alkaline, alkaline-earth, and transition metal ions. There cations provide an electric field inside the pores that prefer to adsorb gas like $CO_2$. Therefore, FAU framework can enhance $CO_2/CH_4$ selectivity **[56-60]**.

### 2.3.2 Method to overcome interfacial defects in MMMs

The major problem in mixed matrix membrane is interfacial defects due to poor compatibility between polymer phase and external fillers surface. The interfacial defects can be classified in to three forms:

a) Interfacial void

The interfacial void defect is caused by polymer contraction from surface of filler. This phenomenon results in an increase in gas permeability but a decrease in the gas selectivity (**Figure 9(a)**).

b) Rigidified polymer

Densification of polymer can cause filler encapsulation. This phenomenon can lead to a polymer rigidified region around filler and result in decreasing the gas permeability with or without an impact on the gas selectivity (**Figure 9(b)**).

c) Pore blockage

The molecule of polymer can pass through the pores of filler and cause a pore blocking. This phenomenon results in decreasing gas permeability and gas selectivity (**Figure 9(c)**).

(a) Interfacial void around the sieve

(b) Rigidified polymer around the sieve

(c) Sieve partial pore blockage
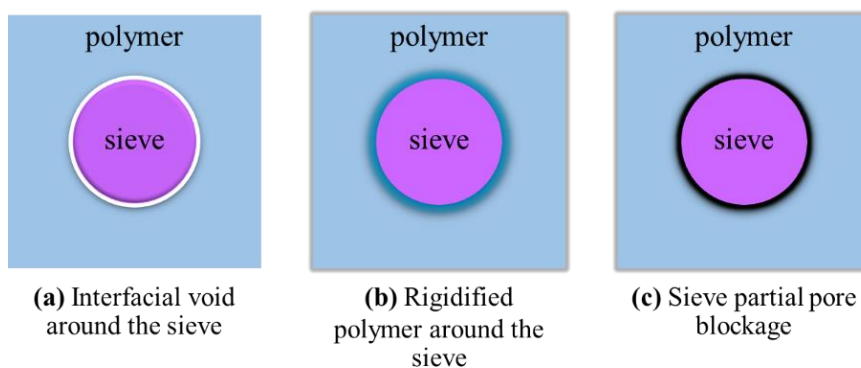
**Figure 9** The interfacial defects schematic: **(a)** interfacial voids, **(b)** rigidified polymer chain, and **(c)** pore blockage

Several methods have been applied to overcome the interfacial defect between polymer and fillers **[61, 62]**. It could be summarized in three main approaches

1. The modification of polymer or filler prior to mixing

This method is mainly focus on the modification of surface fillers and/or polymer chain to increase their compatibility or form the functional group for generating roughness that can promote non-covalent adhesion on fillers surface before mixing the two different phase.

2. Annealing the mixed components

Thermal treatment is applied after forming a membrane. Thermal treatment at the temperature higher than glass transition temperature (Tg) of polymer could provide a better attach of polymer chains on the zeolite surface. However, this method cannot guarantee the defect-free membrane.

3. Gap filling and bridging method

This method is an adding a new component to fill the gap between polymer and fillers. Silane coupling agents were normally used in this route **[63]**. Silane coupling agents act as a bridge connecting polymer and fillers via chemical bonding such as covalent bond and hydrogen bond. Moreover, the hydrophobic nature of silane molecule can reduce the water swelling in polymer. Hence, silane coupling agents lead to an improvement in the interface adhesion and zeolite dispersion **[64, 65]**.

The aminosilane coupling agents were proposed to enhance the polymer and filler adhesion as an integral chain linker **[64, 65]**. The silane groups in the coupling agents can react with the hydroxyl groups (R-OH) of zeolite and the amino group in the coupling agents can react with some functional groups in polymers such as carbonyl group (R−CO−R) **[50]**. The aminosilane grafting process of zeolite Y can be described as follows **[66, 67]**;

Step 1: Hydrolysis reaction of aminosilane coupling agents

Moisture from zeolite surface or water content in organic solvent can react with aminosilane coupling agent and form the silanols group (R−Si−OH).



Step 2: Condensation reaction between aminosilane and aminosilane

The silanols group between aminosilane coupling agent will self-condense and react with hydroxyl groups of zeolite surface via interaction from hydrogen bond (OH−OH) and form siloxane bond on zeolite surface.
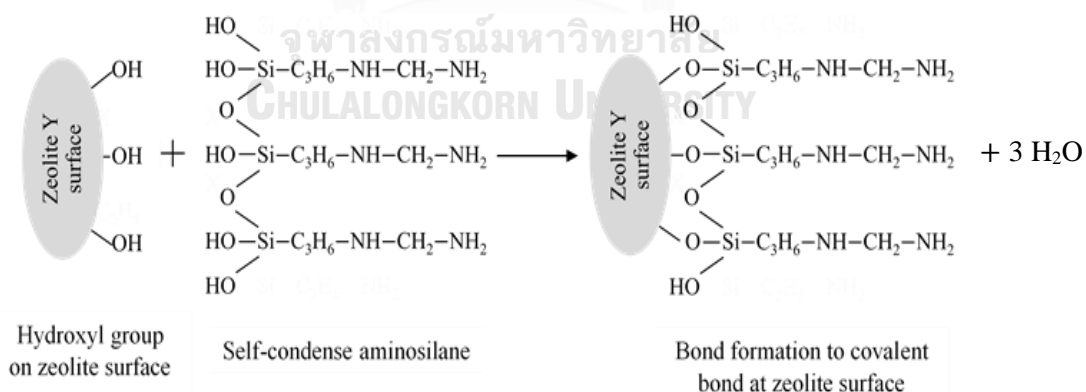


**Figure 10** The connecting between aminosilane coupling agent and fillers in aminosilane grafting process

However, over grafting must be avoid because it will create the new thick layer between zeolite and polymer and increase the mass transfer resistance of the mixed matrix membranes. Therefore, over crosslinking can cause a decrease in

permeability due to rigidified polymer and pore blockage. O. G. Nik et al **[36, 66-68]** studied the effects of reaction parameters on amino-grafted density explained as follows:

Effect of solvent polarity

In nonpolar solvent, hydrogen bond between amine-amine interactions in aminosilane may result in clustering of the aminosilanes that decrease mobility of the aminosilane molecule. Moreover, when the cluster of the aminosilanes reacts with hydroxyl groups of zeolite surface, it will form non-uniform multilayer grafting on the zeolite surface. However, in polar solvents like alcohol it decreased affinity between amine-amine groups. Hydrogen bond of amine-hydroxyl is stronger than amine-amine. On the other hand, it is well known that when silica is exposed to a mono-hydroxyl group such as ethanol, OH groups can cap the Si-OH of zeolite surface. Si-OH on zeolite surface may be converted to $Si-C_2H_5$ by transesterification which is more hydrophobic. This prevents hydrogen bonding between zeolite surface and aminosilane. This resulted in the low aminosilane grafted density and uniform grafted monolayer.

Effect of water content and aminosilane coupling agent concentration

The high contain of water results in self-polymerization of aminosilane and produces a high amount of silane condensation. It will form non-uniform multilayer grafting on zeolite surface. Moreover, when increasing concentration of the aminosilane coupling agent, the density of the grafted aminosilane increased, forming non-uniform multilayer on zeolite surface.

Effect of reaction time and reaction temperature

The density of grafted aminosilane become increased when the reaction time increased. In the same way, the increasing reaction temperature resulted in an increase in reaction rate and aminosilane can better condense on the zeolite surface without a concern for aminosilane self-polymerization in anhydrous solvent.

# CHAPTER 3

# RESEARCH METHODOLOGY

## 3.1 Material

Polysulfone (PSF, MW~22,000 g/mol) and N-[3-(trimethoxysilyl)propyl] ethylenediamine - 97% (AEAPTMS, MW~222.36 g/mol) were bought from Sigma-Aldrich. Polyether-block-amide (Pebax 1657) was purchased from Arkema Inc. N-Methyl-2-Pyrrolidone (NMP, 99%) was obtained from Acros Organics. Ethyl alcohol (EtOH) was bought from Carlo Erba. Zeolite Y-type powder (ZeY) CBV720 was provided by Zeolyst International with 250 nm of particle size and 15 of Si/Al mole ratio (data from the manufacturer).

## 3.2 Grafting of aminosilane on the zeolite

The moisture of ZeY powder was removed by heating at 100 °C overnight in an oven before use. 2 g of dried ZeY powder was added in a round bottom flask combining 100 mL of EtOH (polar medium) and sonicated for 15 min. After that, ZeY suspended EtOH solution was stirred for 1 hr at 85°C before adding 8 mL of AEAPTMS to the slurry. The reaction was carried out under a reflux of nitrogen gas for 24 hr. After that, the grafting reaction was terminated by cooling the slurry to a room temperature. The grafted zeolite was filtered and washed with EtOH several times. Lastly, excess solvent from modified zeolite Y-type (mo-ZeY) was remove by heating at 100°C in an oven overnight.

## 3.3 Membrane fabrication

### 3.3.1 Preparation of support layer

The support layer of hollow fiber membrane was fabricated by a dry-jet/wet quench spinning process. The PSF was dissolved in NMP under a mixing condition at 400 rpm at 65°C to generate homogeneous dope solution with 20 wt% polymer concentration. After that, the PSF solution was left at room temperature and sonicated for 10 min to degas the air trapped in the dope solution.

The prepared solution was added into the dope solution cylinder and distillated water was added into the bore fluid cylinder of extruder. The PSF solution and bore fluid in each cylinder were co-extruded by dry-jet/wet quench spinning process under following condition:

- 10 cm of air gap between spinneret and coagulation bath
- 30°C of extruder temperature
- 1.1 g/min of dope solution mass flowrate
- 0.28 g/min of bore fluid mass flow rate.

The obtain support layer of hollow fiber was kept in distillated water for 2 days and dried overnight in a vacuum oven at 50 °C.

### 3.3.2 Coating procedure of the selective layer on the PSF support

The desired amount of ZeY or mo-ZeY was added in to a mixture solution of EtOH: distilled water (70:30 mass ratio). To ensure the good dispersion of fillers, sonication was applied to the filler suspended solution for 30 min. About 1 wt% of Pebax 1657 was added into the suspension mixture to "prime" the filler for improving the interaction between zeolite and polymer. The slurry was mixed under a stirred at 400 rpm at 65 °C to form a homogeneous solution. After the priming step, the remaining amount of Pebax was added into the prime solution form 5 wt% of Pebax. Finally, 10 min of sonication was applied for degassing the air trapped in the solution and to ensure the dispersion of the fillers.

The prepared coating solution containing Pebax and desired amount of fillers was added into a glass cylinder. After that, the prepared hollow fiber support was dipped into the coating solution for 15 min. Finally, thin coated composite hollow fiber membranes were dried overnight in an oven at 50 °C.

## 3.4 Characterization method

Brunauer-Emmett-Teller (BET, MicrotracBEL Corp. BELSORP-max) was used to characterize surface area and porosity of the fillers with and without surface modification. The properties were determined by $N_2$ adsorption-desorption isotherms under liquid Nitrogen (76 K).

X-Ray Diffraction (XRD, Bruker D8 Advance) method was used to characterize the crystal structure of the prepared fillers and membranes. Copper (Cu) was used to emit λ-rays radiation at wavelength 1.54 Å under 40 kV of accelerating voltage and 4 mA of electric current. The scan angle (2θ) of this test was recorded from 5° to 40° with increment of $0.02°$ $s^{-1}$.

Attenuated total reflectance- Fourier transform infrared spectroscopy (ATR-FTIR, Scientific Nicolet 6700) was used to measure the chemical functional group of the samples. For each specimen, 32 scans were collected with a wavenumber resolution of 4 $cm^{-1}$.

Scanning electron microscope (SEM, Hitachi S-3400N) was used to observe morphology and structure of the fillers and the prepared membranes. The membrane sample was fractured in liquid nitrogen and gold (Au) was coated on the sample by an ion sputter coater (Hitachi E-1010).

Differential scanning calorimetry (DSC, Shimadzu DSC 60A Plus) was used to investigate the glass transition temperature (Tg) and melting enthalpy ($\Delta H_c$) of membranes. The results were analyzed at a temperature range from -100 to 250 °C with a heating rate of 10 °C/min in $N_2$ ambient.

## 3.5 Membrane performance test

Hollow fiber membranes were packed in a stainless-steel module with 40 mm inside diameter by using an epoxy glue. The membrane module was then attached to the gas permeation apparatus illustrated in **Figure 11**. 20 $cm^3$/min of $CO_2/CH_4$ (50:50 mol ratio) gas mixture was fed from the shell side of membrane module, while helium was fed from the tube side of the membrane module to carry permeate gas to the gas chromatography (GC, Shimadzu GC-14B) and film flow meter (Horiba Stec VP-2) at 30 °C. All prepared composite membranes were tested at the steady state and isothermal conditions. The range of temperature and pressure are 30-70 °C and 2-6 bar, respectively
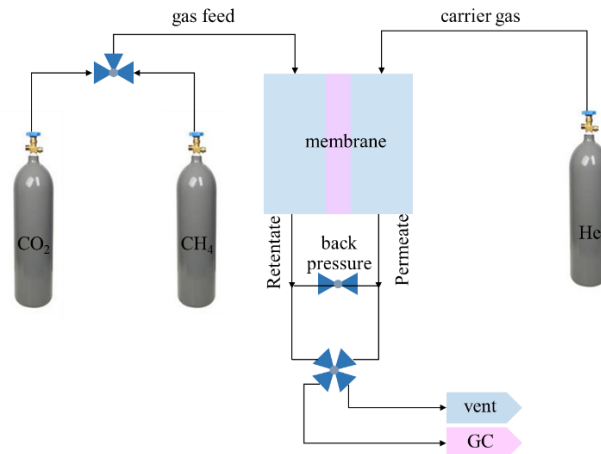
**Figure 11** Gas permeation apparatus diagram

The **Eq3.1** was used to determine the permeability of $CO_2$ and $CH_4$ in gas mixture in Barrers unit, where 1 barrers = $10^{-10}$ $cm^3$ (STP).cm/$cm^2$.s.cmHg.

$$\mathcal{P}_i = \frac{J_i \ell}{(p_{i,0} - p_{i,x})} \qquad \textbf{Eq3.1}$$

Where $\mathcal{P}_i$ = component $i$ gas permeability

$J_i$ = component $i$ gas flux

$p_{i,0} - p_{i,x}$ = transmembrane pressure of component $i$

$\ell$ = membrane thickness

For the gas mixture, gas selective separation factor of membrane is defined as **Eq3.2**

$$\alpha_{ij} = \frac{(y_i / y_j)}{(x_i / x_j)} \qquad \textbf{Eq3.2}$$

Where $\alpha_{ij}$ = component $i$ membrane selective factor

$y_i$ = component $i$ mol fraction in permeate side

$y_j$ = component $j$ mol fraction in permeate side

$x_i$ = component $i$ mol fraction in retentate side

$x_j$ = component $j$ mol fraction in retentate side

# CHAPTER 4

# RESULTS AND DISCUSSION

## 4.1 Filler characterization

In this section, physical and chemical properties such as morphology, chemical structure, crystallinity, and porosity properties of fillers were investigated.
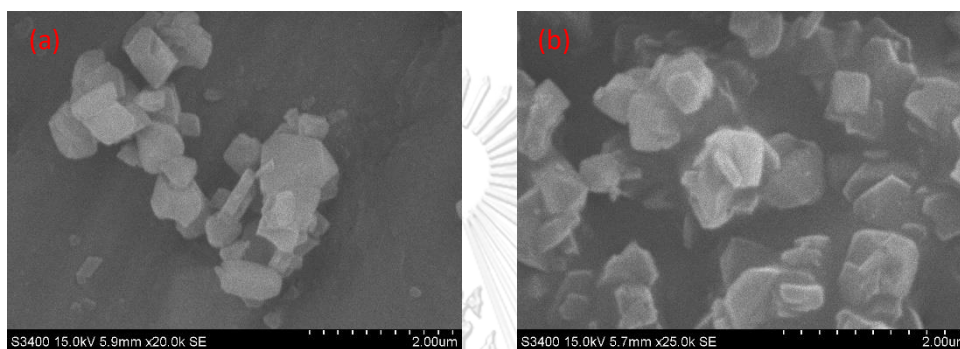


**Figure 12** The scanning electron microscopy (SEM) image of **(a)** zeolite Y (ZeY) and **(b)** the modified zeolite Y (mo-ZeY) with aminosilane

The morphology of zeolite Y (ZeY) and modified zeolite Y (mo-ZeY) powder are showed in **Figure 12 (a)** and **(b)**. The average particle size of ZeY was about 506±118 nm. The particle size of the modified zeolite was measured to be around 509±107 nm, considerably insignificant change from the pristine zeolite.

The ATR-FTIR was used to confirm whether the aminosilane was successfully introduced on the zeolite or not. This work used N-[3-(trimethoxysilyl)propyl] ethylenediamine (AEAPTMS) as the grafting agent. The chemical structure of coupling agent and its reaction on the zeolite are demonstrated in **Figure 13** and **Figure 14**, respectively.
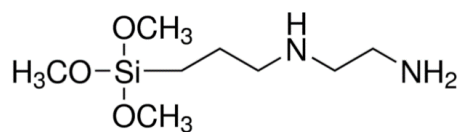
**Figure 13** The chemical formula of [3-(2 Aminoethylamino)propyl]trimethoxysilane (AEAPTMS)
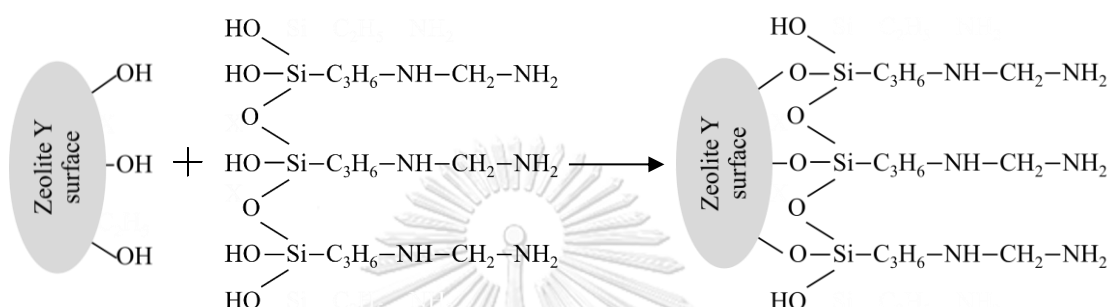


**Figure 14** The condensation reaction step between zeolite Y surface and AEAPTMS

The silanols groups between AEAPTMS could undergo a self-condensation and reacted with hydroxyl groups of zeolite surface, forming siloxane bond (Si-O-Si) on zeolite surface (the other steps of the grafting can be found in chapter 2 section 2.3.2).
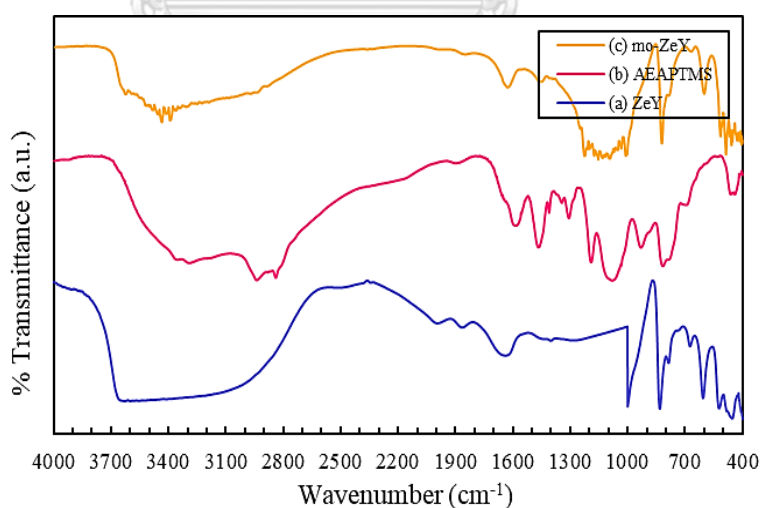


**Figure 15** ATR-FTIR spectra of (a) unmodified ZeY, (b) di-aminosilane coupling agent, and (c) aminosilane grafted ZeY

From the FTIR spectrum of ZeY (**Figure 15 (a)**), the peak at 450 cm$^{-1}$ was referred to Si−O−Al stretching, the peak at 600 and 1000 cm$^{-1}$ were contributed to internal and external tetrahedral symmetrical stretching of Si−O of the ZeY, respectively. While the peak region at around 3000-3600 cm$^{-1}$ was assigned to hydroxyl group (O−H) in sodalite cage in ZeY structure **[69]**.

From FTIR spectrum of the aminosilane grafted zeolite Y (**Figure 15(c)**), the peak at 1470 and 1600 cm$^{-1}$ were assigned to N−H bending and −NH$_2$ scissoring from AEAPTMS molecule, respectively. Base on **Figure 4.13**, the silanol group (Si−OH) between AEAPTMS molecule will self-condense and react with hydroxyl group (O−H) on pristine ZeY surface and from siloxane bond (Si−O−Si) and siloxane linkage on ZeY surface (Si−O−ZeY). So, the bands at about 1030, 1055, 1100, and 1150 cm$^{-1}$ were referred to siloxane bond and siloxane linkage from grafting reaction **[65, 70, 71]**. In addition, the detection of peaks at 3350 and 3410 cm$^{-1}$ was contributed to the primary amine (−NH$_2$) from AEAPTMS molecule. Moreover, the peak from the vibration of hydroxyl reduced due to the stretching of primary amine absorption at the same frequency (around 3300-3500 cm$^{-1}$) **[65, 70]**. This implied that AEAPTMS was successfully grafted on zeolite surface.

Furthermore, X-ray diffractometer was used to investigate the crystallite structure of zeolite Y before and after the modification as shown in **Figure 16**.
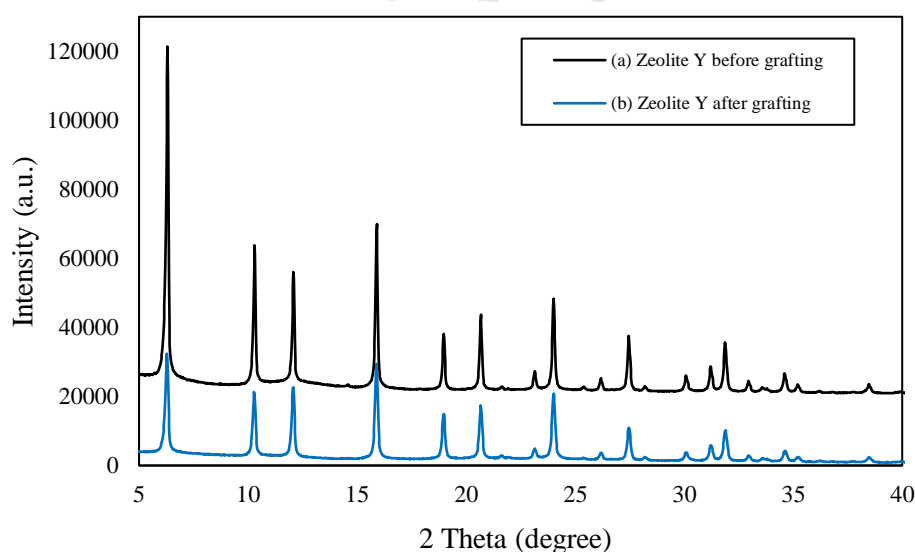


**Figure 16** XRD pattern of zeolite Y **(a)** before grafting and **(b)** after grafting

The XRD technique was used to determine the crystalline structure of the zeolite Y before and after the modification. **Figure 16** shows the XRD patterns of the zeolite Y with and without surface modification. The characteristic peaks at two theta (2θ) equal to 6.3°, 10.3°, 12°, 15.9°, 19°, 20.7°, 24°, 27.5° and 32.1° were identified for both pristine zeolite Y and the modified one **[65]**. However, after the modification, the peak intensity at 6.3° (HLK plane = 1,1,1) and 10.3° (HLK plane = 2,2,0) was significantly reduced. This was due to bonding between Si from the grafting agent and O in these planes. The grafted aminosilane resulted in an increased distance between O and O in the plane.

The porosity properties of zeolite Y before and after grafting from BET characterization are summarize in **Table 3**

**Table 3** BET characterization data of particle

| Properties | Unit | Zeolite Y | Modified zeolite Y |
|---|---|---|---|
| Particle size | nm | 506 | 509 |
| BET surface area | $m^2/g$ | 750 | 305 |
| Total pore volume | $cm^3/g$ | 0.40 | 0.20 |
| Average pore diameter | nm | 2.32 | 1.88 |

The BET surface area, pore volume, and pore diameter of zeolite Y reduced after it was modified. The total pore volume also reduced from 0.40 $cm^3/g$ to 0.20 $cm^3/g$. The mean pore diameter reduced from 2.32 nm to 1.88 nm. The reduction in surface area, pore size, and total pore volume in the modified zeolite was caused by the AEAPTES grafted on the pore wall. These porosity properties were consistent with the XRD characteristic previously mentioned the pore narrowing of the filler after the modification.

## 4.2 Membrane characterization

The cross-section morphology of polysulfone (PSF) hollow fiber was investigated by a scanning electron microscopy (SEM) as shown in **Figure 17**. The structure of hollow fiber contained a finger-like porous structure at the bottom and a dense structure at the outer surface. The outsize diameter and thickness of PSF support layer hollow fiber were about 650±44.7 μm and 140±31.81 μm, respectively.
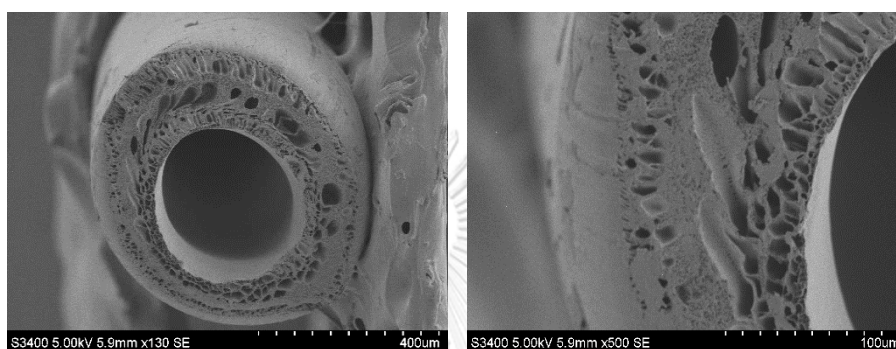


**Figure 17** The cross-section of PSF hollow fiber support layer (left) and close-up cross-section of PSF hollow fiber (right)

The Polyether-block-amide (Pebax) was coated on top of the support fiber, forming the dense selective layer with thickness and surface area of 2.62±0.22 μm and 6.175 cm$^2$, respectively. (see **Figure 4.7**).
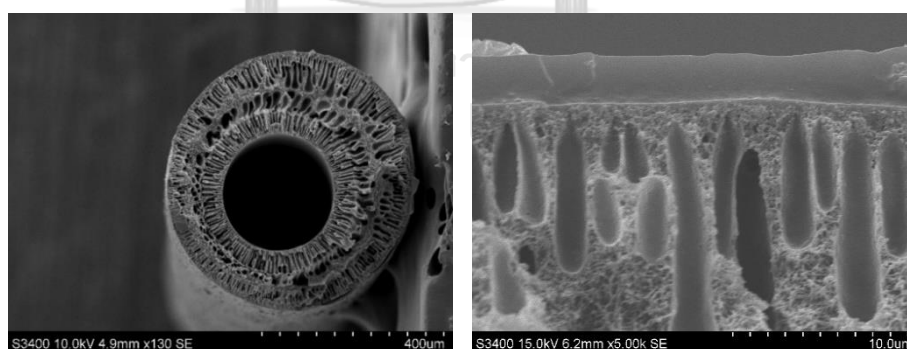


**Figure 18** The cross-section of PSF/Pebax composite membrane (left) and close-up cross-section of PSF/Pebax composite membrane (right)

In the next section, the filler was added into the Pebax matrix in the selective layer, aiming to improve the gas separation performance of the membrane. Effects of fillers on the membrane morphology and properties were investigated.
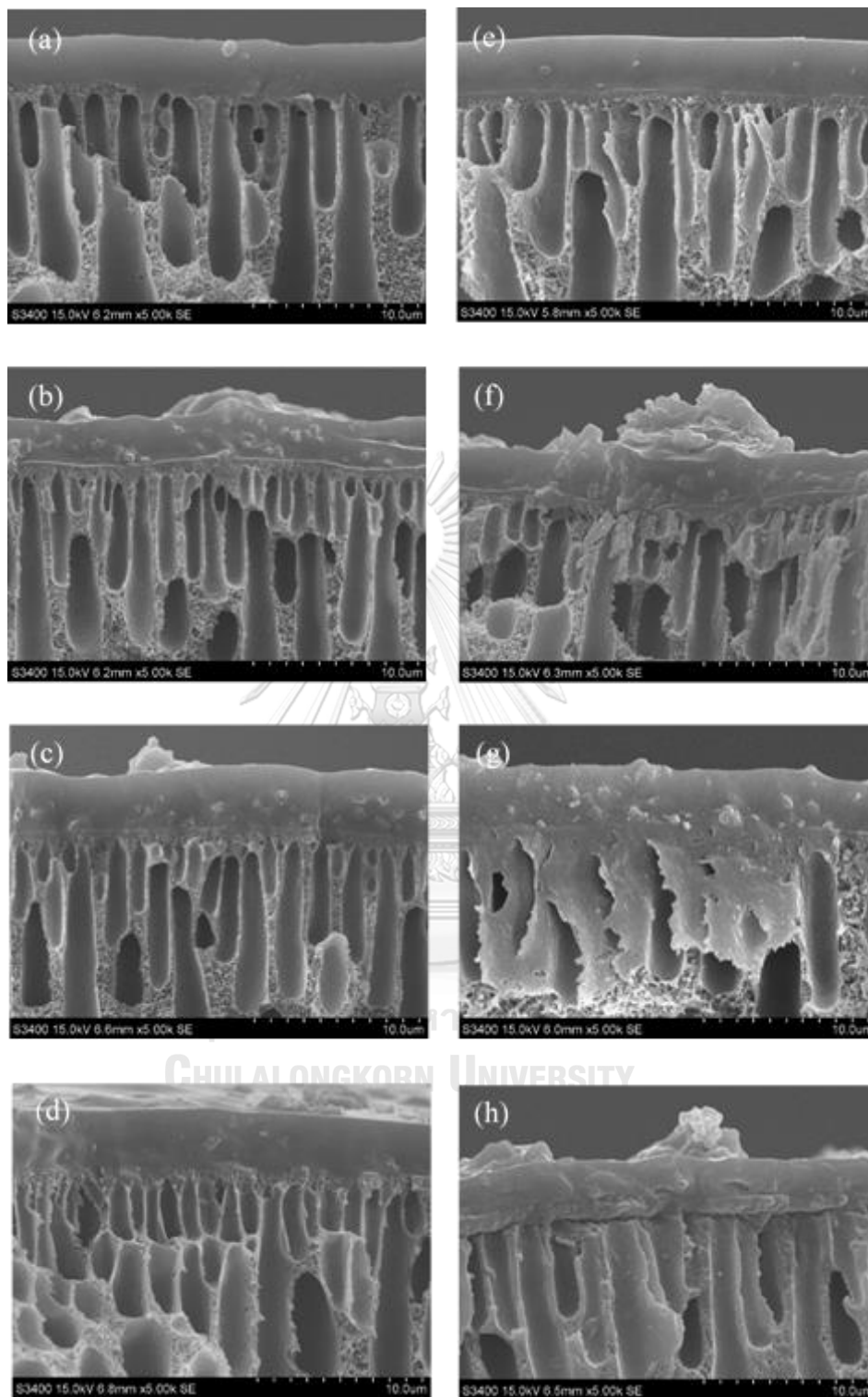
**Figure 19** The cross-section of composite membranes incorporated with **(a)** 5, **(b)** 10, **(c)** 15, and **(d)** 20 wt% of ZeY, respectively, and with **(e)** 5, **(f)** 10, **(g)** 15, and **(h)** 20 wt% of mo-ZeY, respectively.
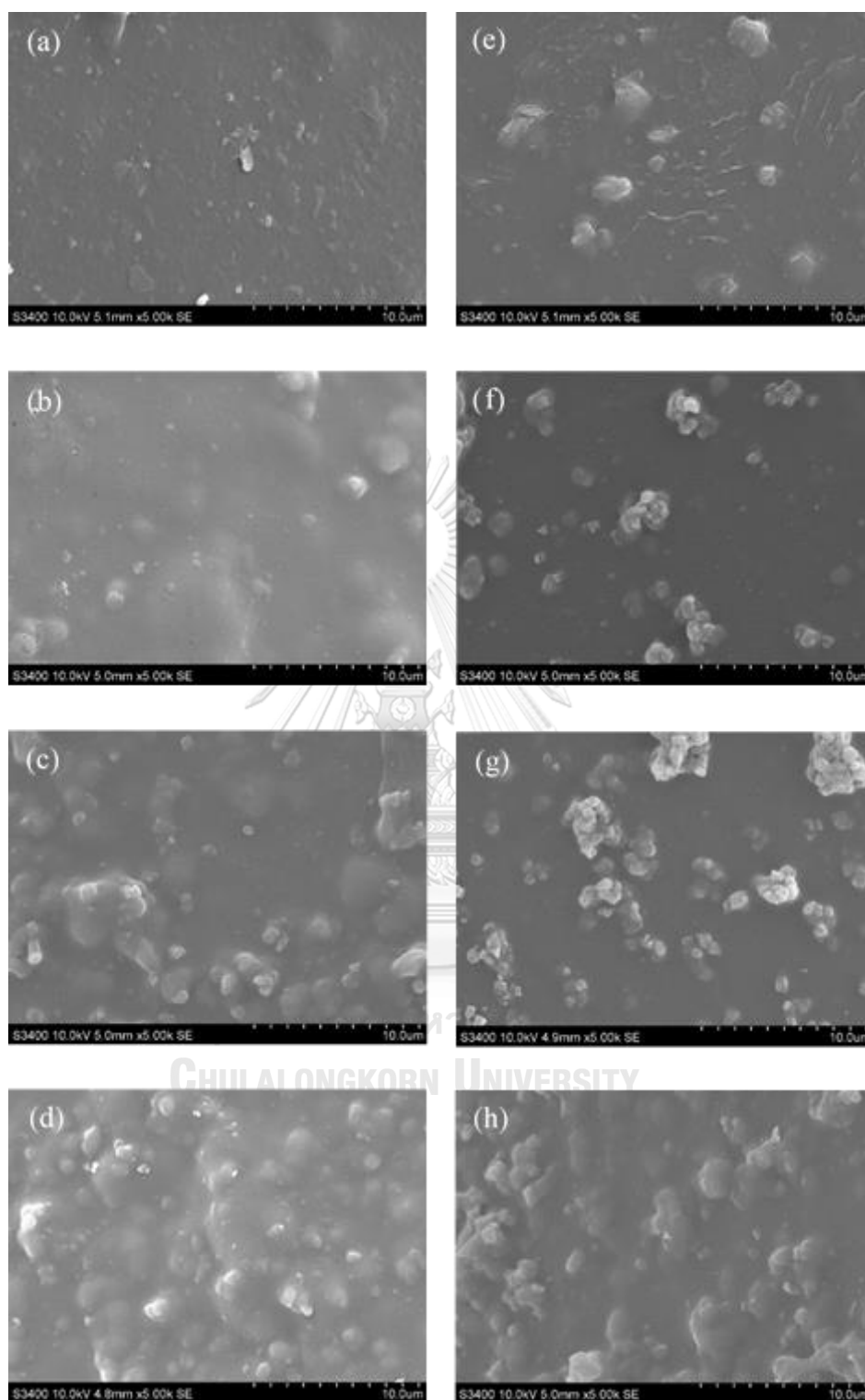
**Figure 20** The top surface of the composite membranes incorporated with **(a)** 5, **(b)** 10, **(c)** 15, and **(d)** 20 wt% of ZeY, respectively, and with **(e)** 5, **(f)** 10, **(g)** 15, and **(h)** 20 wt% of mo-ZeY, respectively.

The mixed matrix membrane (MMM) consists of Pebax as the continuous phase and inorganic filler as disperse phase. The cross-section and top surface morphology of MMM are shown in **Figure 19 (a-h)** and **Figure 20 (a-h)**, respectively. The top layer of all MMMs was dense and integrally coated on the support fiber without an observable interfacial void between fillers and polymer. The average thickness of the selective layer of the prepared MMMs was summarized in **Table 4.** The average thickness of selective layer slightly increased with an increased filler loading. It is worth to mention that when adding more filler, it was more difficult to obtain the uniform coating.

For the MMMs with unmodified zeolite, the SEM image (**Figure 20 (a-d)**) shows that the filler was well dispersed in Pebax phase but started to agglomerate at 10 wt% loading. On the other hand, for MMMs with modified zeolite (**Figure 20 (e-h)**), some filler clusters were found at 15 wt% loading. However, it is worth to mention that though the aggregate was form in both fillers, the aggregated filler cluster still showed fairly good dispersion. In addition, the interfacial gap and void between disperse phase and continuous phase of MMMs did not appeared.

Table 4 The average thickness and surface area of selective layer of MMMs

| MMMs | Thickness of MMMs ($\mu$m) | Area of MMMs ($cm^2$) |
|---|---|---|
| Pebax 1657 + ZeY 5 wt% | 2.83$\pm$0.25 | 6.179 |
| Pebax 1657 + ZeY 10 wt% | 2.94$\pm$0.31 | 6.182 |
| Pebax 1657 + ZeY 15 wt% | 3.05$\pm$0.24 | 6.184 |
| Pebax 1657 + ZeY 20 wt% | 3.09$\pm$0.26 | 6.184 |
| Pebax 1657 + mo-ZeY 5 wt% | 3.16$\pm$0.17 | 6.186 |
| Pebax 1657 + mo-ZeY 10 wt% | 3.16$\pm$0.86 | 6.186 |
| Pebax 1657 + mo-ZeY 15 wt% | 3.30$\pm$0.25 | 6.188 |
| Pebax 1657 + mo-ZeY 20 wt% | 3.29$\pm$0.21 | 6.188 |

To investigate the chemical functional groups of the prepared MMMs, the ATR-FTIR was used. The chemical structure of polysulfone and Pebax are illustrated in **Figure 21** and **22**, respectively.
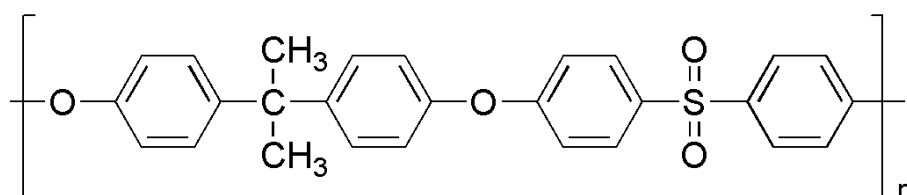
**Figure 21** The chemical formula of polysulfone (PSF)
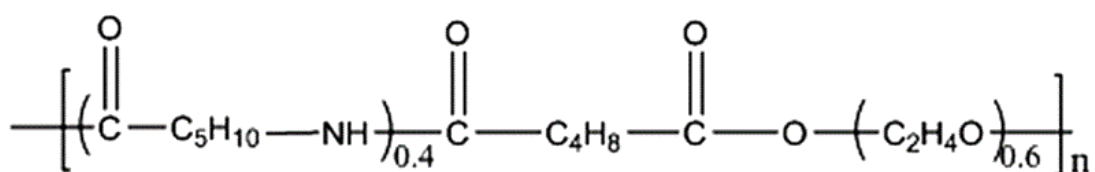


**Figure 22** The chemical formula of Polyether-block-amide (Pebax)
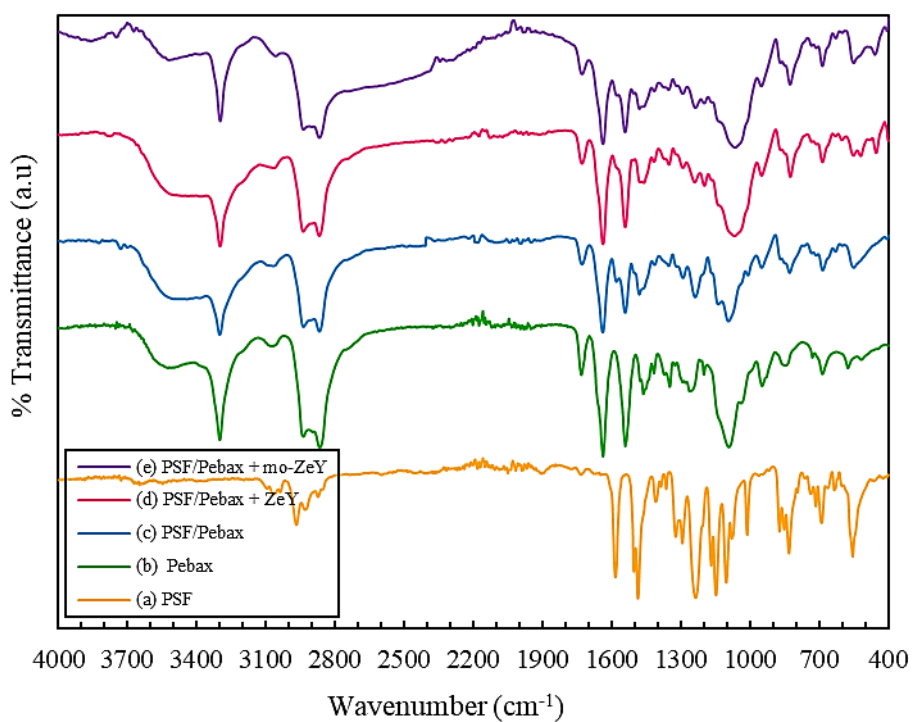


**Figure 23** The ATR-FTIR spectra of (a) PSF support, (b) pristine Pebax, (c) PSF/Pebax CM, (d) PSF/Pebax + 20 %wt ZeY MMM, and (e) PSF/Pebax + 20 wt% mo-ZeY MMM

From **Figure 23**, the prominent peaks of chemical functional group in polysulfone support spectra are observed in stretching spectra **(a)** at 1584, 1236, and 1147 cm$^{-1}$. These characteristic peaks are referred to C=C conjugation in the aromatic ring, C−O between the aromatic ring, and S=O symmetric in the sulfonate group, respectively **[28]**.

From spectra **(b)**, the major stretching vibration of chemical functional group in Pebax membrane are observed at 3300-3400, 1638, 1541, and 1731 cm$^{-1}$ that indicated to secondary amine (=N−H) and N−H region, amide bonding (−CONH), carbonyl group (C=O) in polyamide (PA) section, and carbonyl group (C−O) in polyethylene oxide (PEO) section, respectively **[72]**.

The spectra of all composite membranes **(c-e)** showed the same characteristic peaks as those of pristine Pebax. It indicated that the selective layer was successfully coated on the PSF fiber support. For the MMM from Pebax/ZeY and Pebax/mo-ZeY (**d** and **e**), the wavenumber at 450 and 600 cm$^{-1}$ was observed, which to Si−O−Al and Si−O of the zeolite Y, respectively.

In the case of Pebax/mo-ZeY **(e)**, the IR peak indicating the amine group of grafted zeolite Y was expected; however, this peak overlapped the peak of amine group in Pebax. Moreover, the bands of siloxane bond (Si−O−Si) and siloxane linkage (Si−O−ZeY) at about 1030, 1055, 1100, and 1150 cm$^{-1}$ also overlapped those bands of Pebax.

To trace the change in crystalline property of the polymer matrix after incorporating the filler, the selective layer was coated on a glass slide and subjected to the XRD analysis. Moreover, the selective layer was scraped from the glass slide for differential scanning calorimetry (DSC) analysis for investigate the glass temperature transition (Tg). From XRD characterization, the percent of crystalline degree can be calculated from **Eq.4.1 [40]**. The crystalline structure of Pebax is a semi-crystalline, composing a crystalline region (mainly from PA) and an amorphous region (mainly from PEO). The sharp peaks at two theta (2θ) equal to 24.01° referred to the crystalline while the broad peaks from 13.7° to 21.0° referred to the amorphous section. **[40, 73]**.

$$\%_C = \frac{X_C}{X_C + X_A} \times 100 \qquad \textbf{Eq4.1}$$

Where $\%_C$ = percent of crystalline degree in MMM

$X_C$ = area under the crystalline region in XRD pattern

$X_A$ = area under the amorphous region in XRD pattern

The degree of rigidify, and crystallinity of prepared membranes are compared in **Table 5**.

**Table 5** Crystallization properties of prepared membranes with ZeY and mo-ZeY loading.

| MMMs | Tg (°C) | $\%_C$ (%) |
|---|---|---|
| Pebax | -54.81 | 10.18 |
| Pebax/ 5 wt% ZeY | -54.63 | 10.41 |
| Pebax/ 10 wt% ZeY | -54.08 | 14.55 |
| Pebax/ 15 wt% ZeY | -53.62 | 15.31 |
| Pebax/ 20 wt% ZeY | -52.55 | 18.92 |
| Pebax/ 5 wt% mo-ZeY | -54.48 | 10.85 |
| Pebax/ 10 wt% mo-ZeY | -54.03 | 14.88 |
| Pebax/ 15 wt% mo-ZeY | -53.40 | 15.49 |
| Pebax/ 20 wt% mo-ZeY | -51.80 | 19.02 |

As can be see that, after incorporated filler into the polymer matrix, the percent of crystalline degree increased. This might be explained by H-bond forming between filler surface and polymer chain **[74]** restricting Pebax chain mobility and reducing its flexibility. Moreover, the decrease of crystal content when compare with 100% crystalline state in DSC technique caused by H-bond between polymer and filler that prevents H-bond self-forming in soft and hard section. The interaction between polymer and filler decrease the fractional free volume (FFV) in polymer backbone more than self-forming interaction. The Pebax matrix rigidification after filler loading was observed in this experimental.

## 4.3 Gas separation performance of membrane

The gas separation performance of the prepared composite hollow fiber membranes was tested with a gas mixture of $CO_2$ and $CH_4$ (50:50 mol ratio) at the constant feed flow rate at 20 $cm^3$/min at 30°C. Various pressures from 2-6 bar and temperature 30-70 °C were applied. The effects of filler loading from zeolite Y and modified zeolite Y on membrane performance were investigated. The separation behavior at various pressure and temperature were observed.

### 4.3.1 Effect of filler loading

The effects of zeolite Y and modified zeolite Y loading on the separation performance of mixed matrix composite membrane were summarized in **Table 6** and shown in **Figure 24** and **25**.

**Table 6** The effect of ZeY and mo-ZeY loading on the $CO_2$ and $CH_4$ permeability and $CO_2/CH_4$ selectivity. The separation performance was tested at pressure 2 bar and 30 °C of temperature

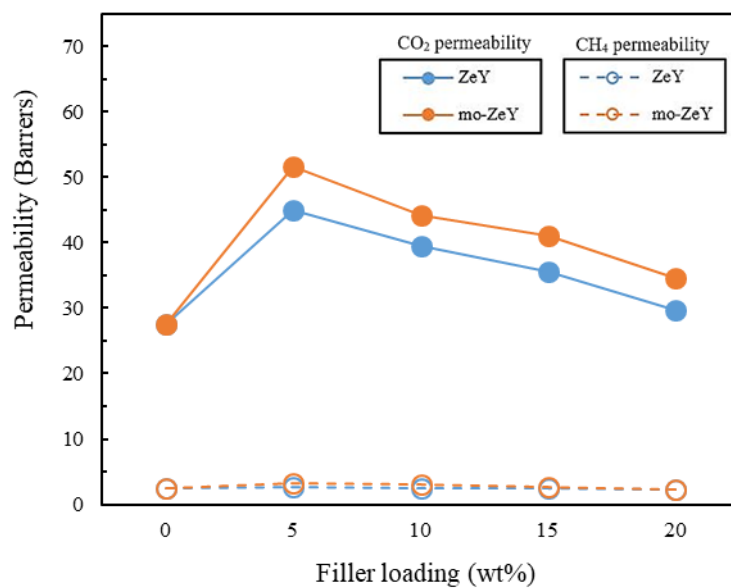| MMM | filler loading (%wt) | $CO_2$ permeability (Barrers) | $CH_4$ permeability (Barrers) | $CO_2/CH_4$ selectivity |
|---|---|---|---|---|
| | 0 | 27.48 | 2.37 | 10.97 |
| | 5 | 45.05 | 2.63 | 19.82 |
| **ZeY** | 10 | 39.45 | 2.52 | 16.84 |
| | 15 | 35.50 | 2.39 | 14.2 |
| | 20 | 29.70 | 2.23 | 11.59 |
| | 0 | 27.48 | 2.37 | 10.97 |
| | 5 | 51.73 | 3.32 | 21.53 |
| **mo-ZeY** | 10 | 44.13 | 3.12 | 19.85 |
| | 15 | 41.12 | 2.64 | 19.68 |
| | 20 | 34.58 | 2.20 | 19.5 |

**Figure 24** The effect of ZeY and mo-ZeY loading on the $CO_2$ and $CH_4$ permeability. The prepared membranes were tested at 2 bar and 30 °C (solid line for $CO_2$ and dash line for $CH_4$).
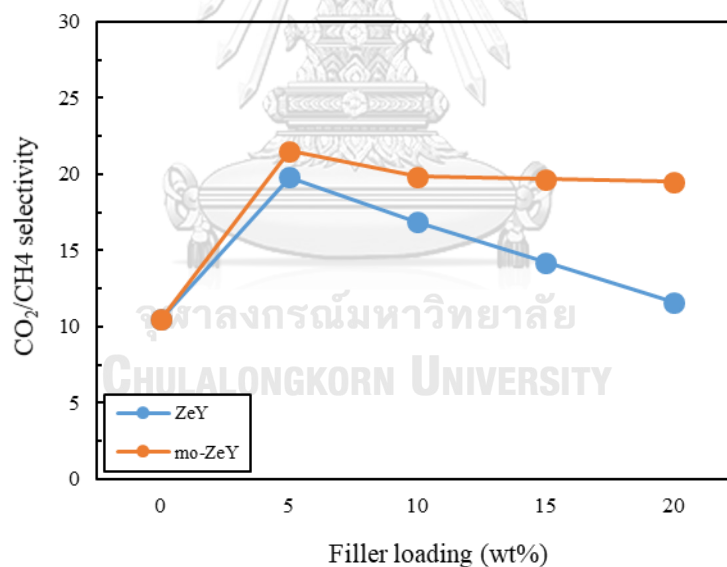


**Figure 25** The effect of ZeY and mo-ZeY loading on the $CO_2/CH_4$ selectivity. The prepared membranes were tested at 2 bar and 30 °C

It was well known that gas separation in polymeric membranes is contributed to polymer structure. The presence of carbonyl group in PEO section and amine group in PA section promoted the permeation of $CO_2$ via dipole induced dipole force.

The addition of ZeY and mo-ZeY provided a positive impact on membrane performance. The gas transport in membranes could be enhanced by the presence of zeolite framework. The $CO_2$ molecule can diffuse through the filler pores easier than $CH_4$. This is because the cations in aluminosilicate framework providing a good better electrostatic interaction for the $CO_2$ [56-60].

At the same filler loading, the membranes with mo-ZeY resulted in a better separation performance compared to ZeY/Pebax membrane (**Figure 24** and **25**). That could be because of the amino group on zeolite Y surface that enhanced the interaction with $CO_2$. Moreover, the typical dry process $CO_2$ chemisorption mechanism was presented for primary amine ($-NH_2$) is as follow [65];

$$CO_2 \ + \ 2RNH_2 \ \rightleftharpoons \ RNHCO_2^- \ + \ RNH_3^+$$

$RNH_2$ (primary amine) on zeolite Y surface can reacted with $CO_2$ forming $RNHCO_2^-$ (carbamate ions). $RNH_2$ is a facilitate transport of $CO_2$ molecule by solution and diffusion through the matrix of Pebax.

The decrease in membranes performance was obtained for MMMs with increasing filler loading from 5 to 20 wt% due to the filler agglomeration that formed the non-selective path from an intrapore among the aggregated particles. Moreover, a decreasing of gas permeability might also be filler pore blocked by Pebax that the effect of pore clogged might be accompanied rigidification of polymer matrix. Moreover, the filler particle in Pebax matrix disturbed the polymer chain mobility and reduce flexibility in backbone [65, 72, 75]. From both reason can be explained from degree of crystallinity of membrane. So, it can be referred that the filler addition into polymer matrix can be enhanced the performance of membrane.

From these reason can be explained from DSC characterization of membrane section. The increasing of Tg also shown that the Pebax matrix rigidification in polymer chain. So, it can be concluded that 5 wt% is the best loading in this work. It

can be provided the highest membrane performance because it provides good dispersion and compatibility between Pebax and filler.

### 4.3.2 Effect of pressure

The effects of pressure on the separation performance of pristine Pebax membrane and the MMMs with 5 wt% ZeY and 5 wt% mo-ZeY were summarized in **Table 7** and compared in **Figure 26** and **27**.

**Table 7** The effect of pressure on the $CO_2$ and $CH_4$ permeability and $CO_2/CH_4$ selectivity at 30 °C of temperature and 5 wt% of filler loading and neat Pebax.

| MMM | Pressure (bar) | $CO_2$ permeability (Barrers) | $CH_4$ permeability (Barrers) | $CO_2/CH_4$ selectivity |
|---|---|---|---|---|
| Neat Pebax | 2 | 27.48 | 1.76 | 10.97 |
| | 3 | 26.96 | 1.73 | 13.12 |
| | 4 | 22.32 | 1.44 | 17.07 |
| | 5 | 19.96 | 1.28 | 20.09 |
| | 6 | 18.08 | 1.15 | 23.07 |
| 5 wt% ZeY | 2 | 45.06 | 2.88 | 19.82 |
| | 3 | 38.07 | 2.44 | 23.15 |
| | 4 | 36.44 | 2.33 | 24.09 |
| | 5 | 28.98 | 1.85 | 29.38 |
| | 6 | 26.27 | 11.43 | 6.65 |
| 5 wt% mo-ZeY | 2 | 51.72 | 3.31 | 21.53 |
| | 3 | 43.47 | 2.78 | 25.88 |
| | 4 | 41.32 | 2.64 | 28.05 |
| | 5 | 37.70 | 2.01 | 31.37 |
| | 6 | 30.95 | 11.10 | 8.74 |
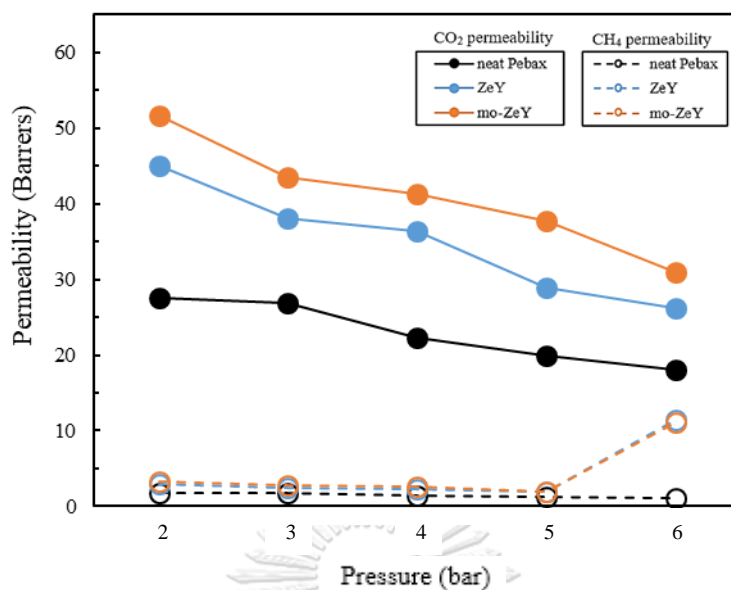
**Figure 26** The effects of pressure on the $CO_2$ and $CH_4$ permeability of the membrane from neat Pebax and MMMs with 5 wt% of ZeY and mo-ZeY at 30 °C of temperature (solid line for $CO_2$ and dash line for $CH_4$).



**Figure 27** The effect of pressure on the $CO_2/CH_4$ selectivity of the membrane from neat Pebax and MMMs with 5 wt% of ZeY and mo-ZeY at 30 °C of temperature.

When increasing the feed pressure from 2 to 5 bars, the $CO_2$ permeability of all membranes tended to decrease but $CO_2/CH_4$ selectivity tended to increase. This might be due to a compaction of polymer structure that caused a reduction of the free volume in polymer matrix and restricted the transport of $CO_2$ and $CH_4$. However, this affected the transportation of $CH_4$ more than $CO_2$. As the result, the $CO_2/CH_4$ selectivity was enhanced when increasing the pressure **[65, 72, 75]**.

However, when increasing the pressure to 6 bars, the gas permeability tended to increase but $CO_2/CH_4$ selectivity tended to decrease in mixed matrix composite membranes case. The gas solubility was increase may be the pressure at 6 bar is initiation pressure of $CO_2$-plasticization and cause the loose of polymer chain. So, membrane stability should be tested for future work.

The results revealed that the pressure at 2 bar is suitable for this application because it can provide a high $CO_2$ permeability and $CO_2/CH_4$ selectivity.

จุฬาลงกรณ์มหาวิทยาลัย

CHULALONGKORN UNIVERSITY

### 4.3.3 Effect of operating temperature

The effects of operating temperature on the separation performance of neat Pebax and mixed matrix composite membrane were summarized in **Table 8** and shown in **Figure 28** and **29**.

**Table 8** The effect of operating temperature on the $CO_2$ and $CH_4$ permeability and $CO_2/CH_4$ selectivity at 2 bar of pressure and 5 wt% of filler loading and neat Pebax.

| MMM | temperature (°C) | $CO_2$ permeability (Barrers) | $CH_4$ permeability (Barrers) | $CO_2/CH_4$ selectivity |
|---|---|---|---|---|
| Neat Pebax | 30 | 27.41 | 1.76 | 10.97 |
| | 40 | 39.98 | 4.56 | 9.81 |
| | 50 | 46.24 | 6.68 | 9.02 |
| | 60 | 55.96 | 9.96 | 7.65 |
| | 70 | 67.47 | 13.13 | 5.52 |
| ZeY | 30 | 45.06 | 2.88 | 19.82 |
| | 40 | 54.85 | 5.46 | 12.91 |
| | 50 | 60.00 | 7.13 | 11.51 |
| | 60 | 63.28 | 9.37 | 9.85 |
| | 70 | 72.02 | 12.54 | 7.51 |
| mo-ZeY | 30 | 51.72 | 3.31 | 21.53 |
| | 40 | 65.88 | 5.31 | 16.71 |
| | 50 | 67.21 | 7.30 | 14.60 |
| | 60 | 70.74 | 9.61 | 12.47 |
| | 70 | 77.37 | 12.55 | 9.35 |
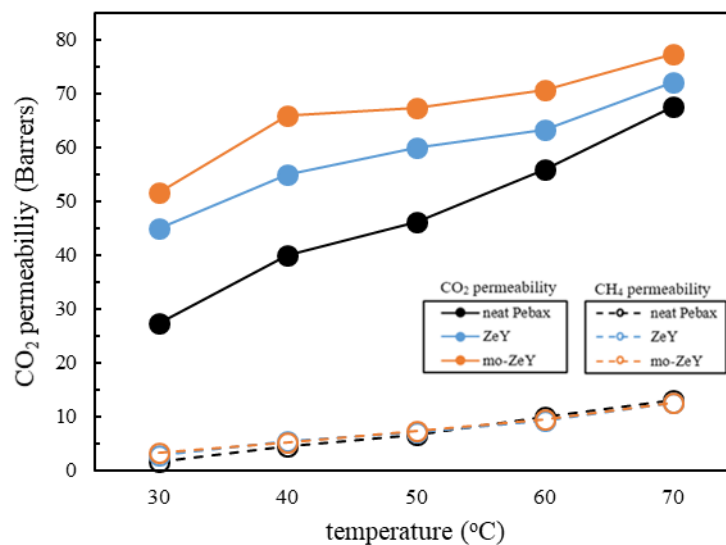
**Figure 28** The effects of operating temperature on the $CO_2$ and $CH_4$ permeability of the membrane from neat Pebax and MMCMs with 5 wt% of ZeY and mo-ZeY at 2 bar (solid line for $CO_2$ and dash line for $CH_4$).



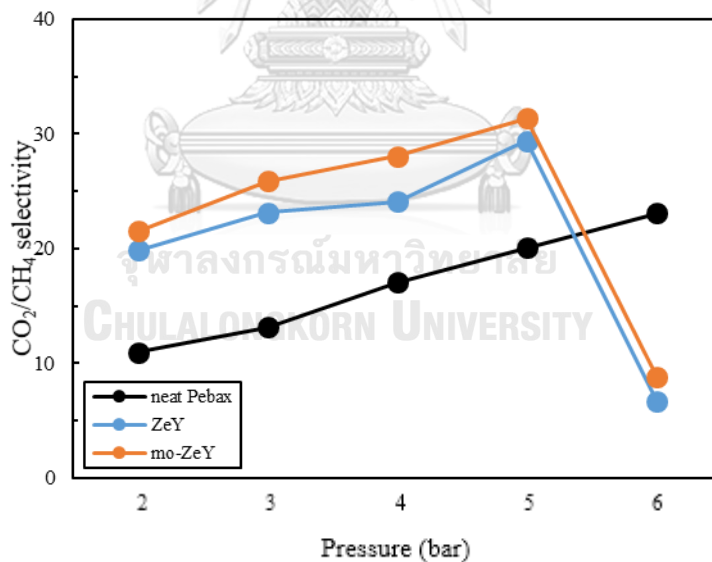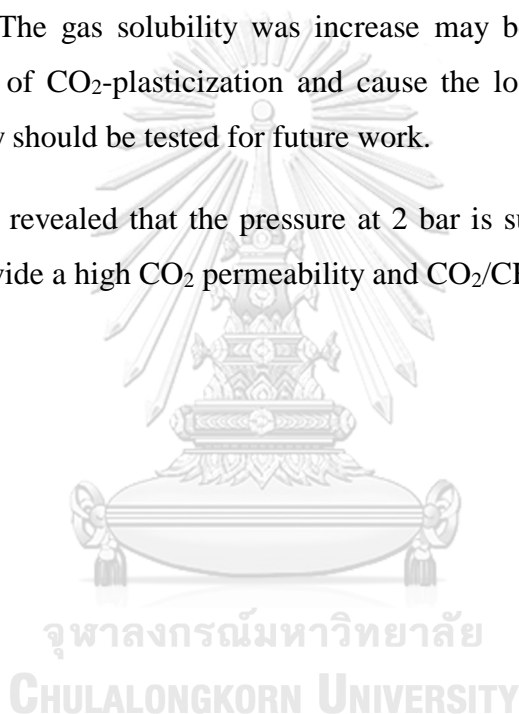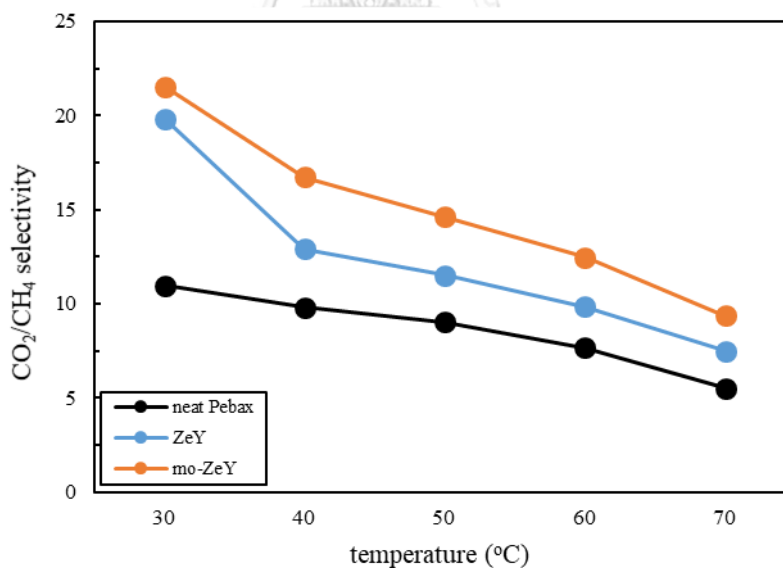**Figure 29** The effect of operating temperature on the $CO_2/CH_4$ selectivity of the membrane from neat Pebax and MMCMs with 5 wt% of ZeY and mo-ZeY at 2 bar

**Figure 28** and **29** show the influence of operating temperature on the gas permeability and $CO_2/CH_4$ selectivity. When operating temperature was raised from 30 to 70 °C, the $CO_2$ permeability increase but $CO_2/CH_4$ selectivity decreased in all various prepared membranes. The increased thermal energy made polymer chain more flexible created more free cavities that promoted the transport of $CO_2$ and $CH_4$ **[76]**. The results revealed that operating temperature at 30-40 °C which is the ambient temperature range of Thailand is suitable for this work.

# CHAPTER 5

## CONCLUSIONS AND RECOMMENDATIONS

This chapter has the two main sections, including conclusions, and recommendation for future work. The objective of this thesis was to develop the mixed matrix composite membranes (MMCMs) for $CO_2/CH_4$ separation base on mixed matrix selective layer of Pebax 1657 with zeolite Y (ZeY) and modified zeolite Y (mo-ZeY) coated on polysulfone (PSF) support at the fixing of feed flowrate 20 $cm^3$/min and 50:50 mol% of $CO_2$ and $CH_4$. The effects of filler loading, pressure, and operating temperature were investigated for finding the optimum condition for membrane fabrication and operating condition for biogas upgrading application. The result of each factor was summarized below.

## 5.1 Conclusion

### 5.1.1 The effect of filler type and filler loading

In this section, the testing was complete at constant 2 bar and 30 °C of pressure and operating temperature, respectively. The ZeY addition provided a positive impact of membrane separation performance ($CO_2$ permeability and $CO_2/CH_4$ selectivity). When compare with the neat Pebax membrane, the addition of ZeY can improve the $CO_2$ permeability from 27.41 to 36.54 barrers and improve the $CO_2/CH_4$ selectivity from 10.97 to 19.82 at lowest loading. That is because electrostatic filed in zeolite framework can used as a facility in $CO_2$ selectivity and sorption because the $CO_2$ molecule has stronger electrostatic quadrupole and leading to more interacted with cations in zeolite framework more than $CH_4$.

When comparing the ZeY addition at lowest loading and the mo-ZeY addition, the modified filler showed more positive impact on the $CO_2$ permeability and $CO_2/CH_4$ selectivity. That is because the $-NH_2$ immobilized can generate the partial discharge interaction with $CO_2$. However, a decrease in membrane performance was obtained when increasing filler loading due to filler agglomeration Moreover, the high filler content could cause a rigidified of polymer matrix. So, the best filler loading was found at 5 wt% in this study.

### 5.1.2 The effect of pressure

Pressure had a significant impact on membrane separation performance. For all membrane from this work, the increased pressure resulted in a reduction of gas permeability but increasement in $CO_2/CH_4$ selectivity. This might be because of polymer compaction. The pressure at 2 bar is suitable for this work because it can provide a high membrane performance at the lowest energy consumption.

### 5.1.3 The effect of operating temperature

When the operating temperature increase from 30 to 70 °C, the $CO_2$ permeability increase but $CO_2/CH_4$ selectivity decrease in all membranes. The operating temperature at 40 °C is proper for this work because it can provide a high membrane performance and low energy consumption.

## 5.2 Recommendations for the future work

Membrane stability should be tested. In addition, the application of the prepared membrane in real raw biogas containing $H_2S$ and humid is suggested.

# APPENDIX

## APPENDIX A: Membrane effective area calculation

The membrane effective area can be calculated from as follows:

$$A = n\pi(d+2\ell)L$$

Where  A = membrane effective area

n = number of hollow fiber membrane line

d = outside diameter of polysulfone support

$\ell$ = selective layer thickness

L = hollow fiber length

Example membrane effective area calculation

Given: number of hollow fiber membrane line = 10 lines

outside diameter of polysulfone support = 650 μm

selective layer thickness = 2.62 μm

hollow fiber length = 30 cm

$$A = 10 \times \pi \times (650 \times 10^{-6} \text{ m} + (2 \times 2.62 \times 10^{-6} \text{ m})) \times 30 \times 10^{-2} \text{ m} \times \frac{100 \text{ cm}^2}{1 \text{ m}^2}$$

$$A = 61.755 \text{ cm}^2$$

Therefore, membrane effective area = 61.755 cm$^2$

# APPENDIX B: CO₂/CH₄ selectivity and gas permeability calculation

Table B.1 Experimental GC area data

| Data from Gas chromatography | | | | | |
|---|---|---|---|---|---|
| | Feed | | Permeate side | | Retentate side | |
| | $CO_2$ | $CH_4$ | $CO_2$ | $CH_4$ | $CO_2$ | $CH_4$ |
| Area | 1702919 | 1401973 | 29397 | 1021 | 1428624 | 1322908 |
| Area fraction | 0.55 | 0.45 | 0.97 | 0.03 | 0.52 | 0.48 |

The $CO_2$ mol fraction can be calculated from GC area calibration curve equation

$$y = 0.9622x - 0.0208$$

Where y = mol fraction of $CO_2$ only

x = area fraction of $CO_2$ only

Example of $CO_2$ and $CH_4$ mol fraction calculation

**Feed gas**

y of $CO_2$ = 0.9622(0.55) − 0.0208 = 0.51

∴ y of $CH_4$ = 1−0.51 = 0.49

**Permeate side**

y of $CO_2$ = 0.9622(0.97) − 0.0208 = 0.91

∴ y of $CH_4$ = 1−0.91 = 0.09

**Retentate side**

y of $CO_2$ = 0.9622(0.52) − 0.0208 = 0.48

∴ y of $CH_4$ = 1−0.48 = 0.52

The $CO_2/CH_4$ Selectivity can be calculated from **Eq 3.2** in chapter 3

$$\alpha_{ij} = \frac{(y_i \, / \, y_j)}{(x_i \, / \, x_j)}$$

Where $\alpha_{ij}$ = component $i$ membrane selective factor

$y_i$ = component $i$ mol fraction in permeate side

$y_j$ = component $j$ mol fraction in permeate side

$x_i$ = component $i$ mol fraction in retentate side

$x_j$ = component $j$ mol fraction in retentate side

$$\alpha_{ij} = \frac{0.91/0.09}{0.48/0.52} = 10.97$$

Therefore, The $CO_2/CH_4$ Selectivity is 10.97

Table B.2 Volumetric flowrate from experiment

| Data from film flow meter | | | |
|---|---|---|---|
| | Feed | Permeate side | Retentate side |
| Flowrate | 20.62 | 1.80 | 18.82 |

The total gas recording by using a film flow meter. The $CO_2$ and $CH_4$ volumetric flowrate can be calculated from as follows:

$$Q_i = y_i \times Q$$

Where $Q_i$ = $CO_2$ or $CH_4$ volumetric flowrate

$y_i$ = $CO_2$ or $CH_4$ mol fraction

$Q$ = The total gas volumetric flowrate

Example of $CO_2$ and $CH_4$ volumetric flowrate

**Feed gas**

$Q_{CO_2} = 0.51 \times 20.62 \ cm^3/min = 10.51 \ cm^3/min$

$Q_{CH_4} = 0.49 \times 20.62 \ cm^3/min = 10.11 \ cm^3/min$

**Permeate side**

$$Q_{CO_2} = 0.91 \times 1.80 \text{ cm}^3/\text{min} = 1.64 \text{ cm}^3/\text{min}$$

$$Q_{CH_4} = 0.09 \times 1.80 \text{ cm}^3/\text{min} = 0.16 \text{ cm}^3/\text{min}$$

**Retentate side**

$$Q_{CO_2} = 0.48 \times 18.82 \text{ cm}^3/\text{min} = 9.03 \text{ cm}^3/\text{min}$$

$$Q_{CH_4} = 0.52 \times 18.82 \text{ cm}^3/\text{min} = 9.79 \text{ cm}^3/\text{min}$$

For found the gas CO permeability, volumetric flux at permeate side at standard temperature and pressure (STP) and transmembrane pressure can be calculated as follows:

$$J_{i,STP} = \frac{Q_i}{A} \times \frac{T_{STP}}{T}$$

Where $J_{i,STP}$ = $CO_2$ or $CH_4$ volumetric flux at permeate side at STP

$Q_i$ = $CO_2$ or $CH_4$ volumetric flowrate at permeate side

A = membrane effective area

$T_{STP}$ = standard absolute temperature = 273 K

T = operating absolute temperature

Example of $CO_2$ and $CH_4$ volumetric flux calculation

Given: membrane effective area = 61.75 cm$^2$

operating absolute temperature = 303 K

**Permeate side**

$$J_{CO_2,STP} = \frac{1.64 \text{ cm}^3/\text{min}}{61.75 \text{ cm}^2} \times \frac{273 \text{ K}}{303 \text{ K}} = 0.024 \text{ cm}^3(STP)/\text{cm}^2.\text{min}$$

$$J_{CH_4,STP} = \frac{0.16 \text{ cm}^3/\text{min}}{61.75 \text{ cm}^2} \times \frac{273 \text{ K}}{303 \text{ K}} = 0.002 \text{ cm}^3(STP)/\text{cm}^2.\text{min}$$

Example of $CO_2$ and $CH_4$ volumetric flux calculation

Given: transmembrane pressure = 1 bar

**Feed pressure**

$$P_{CO2,\ feed} = 0.51 \times 1 \text{ bar } (\frac{75.006 \text{ cmHg}}{1 \text{ bar}}) = 38.253 \text{ cmHg}$$

$$P_{CO2,\ feed} = 0.49 \times 1 \text{ bar } (\frac{75.006 \text{ cmHg}}{1 \text{ bar}}) = 36.753 \text{ cmHg}$$

At steady state, permeate side no accumulator pressure

**Permeate side pressure**

$$P_{CO2,\ permeate} = 0 \times 1 \text{ bar } (\frac{75.006 \text{ cmHg}}{1 \text{ bar}}) = 0 \text{ cmHg}$$

$$P_{CO2,\ permeate} = 0 \times 1 \text{ bar } (\frac{75.006 \text{ cmHg}}{1 \text{ bar}}) = 0 \text{ cmHg}$$

So, the gas permeability can be calculated from **Eq 3.1** in chapter 3

$$\mathcal{P}_i = \frac{J_i\ \ell}{(p_{i,0} - p_{i,x})}$$

Where $\mathcal{P}_i$ = component $i$ gas permeability

$J_i$ = component $i$ gas flux

$p_{i,0} - p_{i,x}$ = transmembrane pressure of component $i$

$\ell$ = membrane thickness

Example of $CO_2$ and $CH_4$ permeability calculation

Given: feed pressure = 1 bar and permeate side no accumulator pressure

membrane thickness = 2.62 μm

$$\mathcal{P}_{CO_2, \text{ permeate}} = \frac{0.024 \text{ cm}^3(\text{STP})/\text{cm}^2.\text{min}}{38.253 \text{ cmHg} - 0 \text{ cmHg}} \times 2.62 \times 10^{-6} \text{ m} \times \frac{1 \text{ min}}{60 \text{ s}} \times \frac{100 \text{ cm}}{1 \text{ m}}$$

$$\mathcal{P}_{CO_2, \text{ permeate}} = 27.48 \times 10^{-10} \text{ cm}^3(\text{STP}).\text{cm/cm}^2.\text{s.cmHg or Barrer}$$

$$\mathcal{P}_{CO_2, \text{ permeate}} = 27.48 \text{ Barrer}$$

$$\mathcal{P}_{CH_a, \text{ permeate}} = \frac{0.002 \text{ cm}^3(\text{STP})/\text{cm}^2.\text{min}}{36.753 \text{ cmHg} - 0 \text{ cmHg}} \times 2.62 \times 10^{-6} \text{ m} \times \frac{1 \text{ min}}{60 \text{ s}} \times \frac{100 \text{ cm}}{1 \text{ m}}$$

$$\mathcal{P}_{CO_2, \text{ permeate}} = 2.37 \times 10^{-10} \text{ cm}^3(\text{STP}).\text{cm/cm}^2.\text{s.cmHg or Barrer}$$

$$\mathcal{P}_{CO_2, \text{ permeate}} = 2.37 \text{ Barrer}$$

Therefore, $CO_2$ and $CH_4$ permeability are 27.48 Barrers and 2.37 Barrers, respective

# APPENDIX C: calculation of the membrane crystallinity degree

Table C.1 Area under the amorphous and crystalline region in XRD pattern

| Amorphous region | Crystalline region |
|---|---|
| 13684.858 | 1551.570 |

The crystallinity degree can be calculated by **Eq 4.1** in chapter 4

$$\% C = \frac{X_C}{X_C + X_A} \times 100$$

Where $\% C$ = percent of crystalline degree in MMM

$X_C$ = area under the crystalline region in XRD pattern

$X_A$ = area under the amorphous region in XRD pattern

Example of crystallinity degree calculation

$$\% cry = \frac{1551.570}{1551.570 + 13684.858} \times 100 = 10.183\ \%$$

Thus, the crystallinity degree of membrane is 10.183 %

# REFERENCES

1. Jeon, Y.-W. and D.-H. Lee, *Gas membranes for $CO_2/CH_4$ (biogas) separation: a review*. Environmental Engineering Science, 2015. **32**(2): p. 71-85.

2. Ozturk, B. and F. Demirciyeva, *Comparison of biogas upgrading performances of different mixed matrix membranes*. Chemical engineering journal, 2013. **222**: p. 209-217.

3. Chen, Y., et al., *New Pebax®/zeolite Y composite membranes for $CO_2$ capture from flue gas*. Journal of Membrane Science, 2015. **495**: p. 415-423.

4. Goh, P., et al., *Recent advances of inorganic fillers in mixed matrix membrane for gas separation*. Separation and Purification Technology, 2011. **81**(3): p. 243-264.

5. Vinoba, M., et al., *Recent progress of fillers in mixed matrix membranes for $CO_2$ separation: A review*. Separation and Purification Technology, 2017. **188**: p. 431-450.

6. Wu, D., et al., *Scale-up of zeolite-Y/polyethersulfone substrate for composite membrane fabrication in $CO_2$ separation*. Journal of Membrane Science, 2018. **562**: p. 56-66.

7. Scholz, M., T. Melin, and M. Wessling, *Transforming biogas into biomethane using membrane technology*. Renewable and Sustainable Energy Reviews, 2013. **17**: p. 199-212.

8. Lin, H. and B.D. Freeman, *Gas solubility, diffusivity and permeability in poly (ethylene oxide)*. Journal of Membrane Science, 2004. **239**(1): p. 105-117.

9. Ismail, A., et al., *Understanding the solution-diffusion mechanism in gas separation membrane for engineering students*. 2005.

10. Liu, S.L., et al., *Recent progress in the design of advanced PEO-containing membranes for $CO_2$ removal*. Progress in Polymer Science, 2013. **38**(7): p. 1089-1120.

11. Wijmans, J.G. and R.W. Baker, *The solution-diffusion model: a review*. Journal of Membrane Science, 1995. **107**(1): p. 1-21.

12. Issaoui, M. and L. Limousy, *Low-cost ceramic membranes: Synthesis, classifications, and applications*. Comptes Rendus Chimie, 2019. **22**(2): p. 175-187.

13.    Xu, L., et al., *Formation of defect-free 6FDA-DAM asymmetric hollow fiber membranes for gas separations.* Journal of membrane science, 2014. **459**: p. 223-232.

14.    Chung, T.S.N., *Fabrication of hollow-fiber membranes by phase inversion.* Advanced Membrane Technology and Applications, 2008: p. 821-839.

15.    Ren, J., et al., *Development of asymmetric 6FDA-2, 6 DAT hollow fiber membranes for $CO_2/CH_4$ separation: 1. The influence of dope composition and rheology on membrane morphology and separation performance.* Journal of membrane science, 2002. **207**(2): p. 227-240.

16.    Wang, K.Y., et al., *The observation of elongation dependent macrovoid evolution in single-and dual-layer asymmetric hollow fiber membranes.* Chemical engineering science, 2004. **59**(21): p. 4657-4660.

17.    Li, D., R. Wang, and T.-S. Chung, *Fabrication of lab-scale hollow fiber membrane modules with high packing density.* Separation and purification technology, 2004. **40**(1): p. 15-30.

18.    Koros, W., Y. Ma, and T. Shimidzu, *Terminology for membranes and membrane processes (IUPAC Recommendations 1996).* Pure and Applied Chemistry, 1996. **68**(7): p. 1479-1489.

19.    Deng, L. and M.-B. Hägg, *Techno-economic evaluation of biogas upgrading process using $CO_2$ facilitated transport membrane.* International Journal of Greenhouse Gas Control, 2010. **4**(4): p. 638-646.

20.    Zulhairun, A., et al., *High-flux polysulfone mixed matrix hollow fiber membrane incorporating mesoporous titania nanotubes for gas separation.* Separation and Purification Technology, 2017. **180**: p. 13-22.

21.    Mohamad, M.B., Y.Y. Fong, and A. Shariff, *Gas separation of carbon dioxide from methane using polysulfone membrane incorporated with zeolite-T.* Procedia engineering, 2016. **148**: p. 621-629.

22.    Md Nordin, N.A.H., et al., *Facile modification of ZIF-8 mixed matrix membrane for $CO_2/CH_4$ separation: synthesis and preparation.* RSC Advances, 2015. **5**(54): p. 43110-43120.

23.  Guo, X., et al., *Mixed matrix membranes incorporated with amine-functionalized titanium-based metal-organic framework for $CO_2/CH_4$ separation.* Journal of Membrane Science, 2015. **478**: p. 130-139.

24.  Rodenas, T., et al., *Mixed matrix membranes based on NH2-functionalized MIL-type MOFs: Influence of structural and operational parameters on the $CO_2/CH_4$ separation performance.* Microporous and Mesoporous Materials, 2014. **192**: p. 35-42.

25.  Zornoza, B., et al., *Functionalized flexible MOFs as fillers in mixed matrix membranes for highly selective separation of $CO_2$ from $CH_4$ at elevated pressures.* Chemical communications, 2011. **47**(33): p. 9522-9524.

26.  Ahn, J., et al., *Polysulfone/silica nanoparticle mixed-matrix membranes for gas separation.* Journal of Membrane science, 2008. **314**(1-2): p. 123-133.

27.  Kim, S., et al., *Polysulfone and mesoporous molecular sieve MCM-48 mixed matrix membranes for gas separation.* Chemistry of materials, 2006. **18**(5): p. 1149-1155.

28.  Ismail, A., et al., *Direct measurement of rheologically induced molecular orientation in gas separation hollow fibre membranes and effects on selectivity.* Journal of Membrane Science, 1997. **126**(1): p. 133-137.

29.  Zhang, Y., et al., *Mixed-matrix membranes composed of Matrimid and mesoporous ZSM-5 nanoparticles.* Vol. 211. 2003.

30.  Dong, G., H. Li, and V. Chen, *Factors affect defect-free Matrimid® hollow fiber gas separation performance in natural gas purification.* Journal of Membrane Science, 2010. **353**(1): p. 17-27.

31.  Shahid, S. and K. Nijmeijer, *High pressure gas separation performance of mixed-matrix polymer membranes containing mesoporous Fe(BTC).* Journal of Membrane Science, 2014. **459**: p. 33-44.

32.  Anjum, M.W., et al., *Polyimide mixed matrix membranes for $CO_2$ separations using carbon–silica nanocomposite fillers.* Journal of Membrane Science, 2015. **495**: p. 121-129.

33.  Amooghin, A.E., M. Omidkhah, and A. Kargari, *The effects of aminosilane grafting on NaY zeolite–Matrimid® 5218 mixed matrix membranes for $CO_2/CH_4$ separation.* Journal of Membrane Science, 2015. **490**: p. 364-379.

34. Li, X., et al., *Synergistic effect of combining carbon nanotubes and graphene oxide in mixed matrix membranes for efficient $CO_2$ separation.* Journal of Membrane Science, 2015. **479**: p. 1-10.

35. Khan, A.L., et al., *Mixed matrix membranes comprising of Matrimid and − $SO_3H$ functionalized mesoporous MCM-41 for gas separation.* Journal of Membrane Science, 2013. **447**: p. 73-79.

36. Chen, X.Y., et al., *Mixed matrix membranes of aminosilanes grafted FAU/EMT zeolite and cross-linked polyimide for $CO_2/CH_4$ separation.* Polymer, 2012. **53**(15): p. 3269-3280.

37. Bae, T.-H., et al., *Facile High-Yield Solvothermal Deposition of Inorganic Nanostructures on Zeolite Crystals for Mixed Matrix Membrane Fabrication.* Journal of the American Chemical Society, 2009. **131**(41): p. 14662-14663.

38. Hashemifard, S.A., A.F. Ismail, and T. Matsuura, *Effects of montmorillonite nano-clay fillers on PEI mixed matrix membrane for CO2 removal.* Chemical Engineering Journal, 2011. **170**(1): p. 316-325.

39. Jamil, A., P.C. Oh, and A.M. Shariff, *Polyetherimide-montmorillonite mixed matrix hollow fibre membranes: Effect of inorganic/organic montmorillonite on $CO_2/CH_4$ separation.* Separation and Purification Technology, 2018. **206**: p. 256-267.

40. Norahim, N., et al., *Composite Membranes of Graphene Oxide for $CO_2/CH_4$ separation.* Journal of Chemical Technology & Biotechnology.

41. Li, X., et al., *Efficient $CO_2$ Capture by Functionalized Graphene Oxide Nanosheets as Fillers To Fabricate Multi-Permselective Mixed Matrix Membranes.* ACS Applied Materials & Interfaces, 2015. **7**(9): p. 5528-5537.

42. Wu, H., et al., *Facilitated transport mixed matrix membranes incorporated with amine functionalized MCM-41 for enhanced gas separation properties.* Journal of Membrane Science, 2014. **465**: p. 78-90.

43. Surya Murali, R., et al., *Mixed matrix membranes of Pebax-1657 loaded with 4A zeolite for gaseous separations.* Separation and Purification Technology, 2014. **129**: p. 1-8.

44. Robeson, L.M., *The upper bound revisited.* Journal of Membrane Science, 2008. **320**(1): p. 390-400.

45.  Suleman, M.S., K.K. Lau, and Y.F. Yeong, *Plasticization and swelling in polymeric membranes in CO$_2$ removal from natural gas.* Chemical Engineering & Technology, 2016. **39**(9): p. 1604-1616.

46.  Fouladvand, S., *Study of MFI zeolite membrane for CO$_2$ separation*, in *Licentiate thesis / Luleå University of Technology*. 2016: Luleå.

47.  Rabiee, H., et al., *Gas permeation and sorption properties of poly(amide-12-b-ethyleneoxide)(Pebax1074)/SAPO-34 mixed matrix membrane for CO$_2$/CH$_4$ and CO$_2$/N$_2$ separation.* Journal of Industrial and Engineering Chemistry, 2015. **27**: p. 223-239.

48.  Zhao, D., et al., *Poly(amide-6-b-ethylene oxide)/SAPO-34 mixed matrix membrane for CO$_2$ separation.* Journal of Energy Chemistry, 2014. **23**(2): p. 227-234.

49.  Amooghin, A.E., M. Omidkhah, and A. Kargari, *Enhanced CO$_2$ transport properties of membranes by embedding nano-porous zeolite particles into Matrimid® 5218 matrix.* RSC Advances, 2015. **5**(12): p. 8552-8565.

50.  Ebadi Amooghin, A., M. Omidkhah, and A. Kargari, *The effects of aminosilane grafting on NaY zeolite–Matrimid®5218 mixed matrix membranes for CO$_2$/CH$_4$ separation.* Journal of Membrane Science, 2015. **490**: p. 364-379.

51.  Yong, H.H., et al., *Zeolite-filled polyimide membrane containing 2,4,6-triaminopyrimidine.* Journal of Membrane Science, 2001. **188**(2): p. 151-163.

52.  Kusworo, T.D., et al., *THE EFFECT OF TYPE ZEOLITE ON THE GAS TRANSPORT PROPERTIES OF POLYIMIDE-BASED MIXED MATRIX MEMBRANES.* 2008, 2008: p. 10.

53.  Li, Y., et al., *Effects of novel silane modification of zeolite surface on polymer chain rigidification and partial pore blockage in polyethersulfone (PES)–zeolite A mixed matrix membranes.* Journal of Membrane Science, 2006. **275**(1-2): p. 17-28.

54.  Şen, D., H. Kalıpçılar, and L. Yilmaz, *Development of polycarbonate based zeolite 4A filled mixed matrix gas separation membranes.* Journal of Membrane Science, 2007. **303**(1): p. 194-203.

55.     Adams, R.T., et al., *CO₂–CH₄ permeation in high zeolite 4A loading mixed matrix membranes.* Journal of Membrane Science, 2011. **367**(1): p. 197-203.

56.     Frising, T. and P. Leflaive, *Extraframework cation distributions in X and Y faujasite zeolites: A review.* Microporous and Mesoporous Materials, 2008. **114**(1): p. 27-63.

57.     Sanaeepur, H., et al., *A novel Co²⁺ exchanged zeolite Y/cellulose acetate mixed matrix membrane for CO₂/N₂ separation.* Journal of the Taiwan Institute of Chemical Engineers, 2016. **60**: p. 403-413.

58.     White, J.C., et al., *Synthesis of Ultrathin Zeolite Y Membranes and their Application for Separation of Carbon Dioxide and Nitrogen Gases.* Langmuir, 2010. **26**(12): p. 10287-10293.

59.     Zhao, L., et al., *Multilayer polymer/zeolite Y composite membrane structure for CO₂ capture from flue gas.* Journal of Membrane Science, 2016. **498**: p. 1-13.

60.     Ramasubramanian, K., et al., *Fabrication of zeolite/polymer multilayer composite membranes for carbon dioxide capture: Deposition of zeolite particles on polymer supports.* Journal of Colloid and Interface Science, 2015. **452**: p. 203-214.

61.     Klaysom, C. and S. Shahid, *Zeolite-based mixed matrix membranes for hazardous gas removal.* 2019. p. 127-157.

62.     Lydon, M.E., et al., *Structure–Property Relationships of Inorganically Surface-Modified Zeolite Molecular Sieves for Nanocomposite Membrane Fabrication.* The Journal of Physical Chemistry C, 2012. **116**(17): p. 9636-9645.

63.     Calabrese, L., et al., *Effect of silane matrix composition on performances of zeolite composite coatings.* Progress in Organic Coatings, 2016. **101**: p. 100-110.

64.     Junaidi, M.U.M., et al., *The effects of solvents on the modification of SAPO-34 zeolite using 3-aminopropyl trimethoxy silane for the preparation of asymmetric polysulfone mixed matrix membrane in the application of CO₂ separation.* Microporous and Mesoporous Materials, 2014. **192**: p. 52-59.

65. Sanaeepur, H., A. Kargari, and B. Nasernejad, *Aminosilane-functionalization of a nanoporous Y-type zeolite for application in a cellulose acetate based mixed matrix membrane for $CO_2$ separation*. Vol. 4. 2014. 63966-63976.

66. Nik, O.G., X.Y. Chen, and S. Kaliaguine, *Amine-functionalized zeolite FAU/EMT-polyimide mixed matrix membranes for $CO_2/CH_4$ separation*. Journal of Membrane Science, 2011. **379**(1): p. 468-478.

67. Nik, O.G., M. Sadrzadeh, and S. Kaliaguine, *Surface grafting of FAU/EMT zeolite with (3-aminopropyl)methyldiethoxysilane optimized using Taguchi experimental design*. Chemical Engineering Research and Design, 2012. **90**(9): p. 1313-1321.

68. Nik, O.G., B. Nohair, and S. Kaliaguine, *Aminosilanes grafting on FAU/EMT zeolite: Effect on $CO_2$ adsorptive properties*. Microporous and Mesoporous Materials, 2011. **143**(1): p. 221-229.

69. Ahmedzeki, N.S., S. Yilmaz, and B.A. Al-Tabbakh, *Synthesis and Characterization of nanocrystalline zeolite Y*. Al-Khwarizmi Engineering Journal, 2016. **12**(1): p. 79-89.

70. Jusoh, N., et al., *Fabrication of silanated zeolite T/6FDA-durene composite membranes for $CO_2/CH_4$ separation*. Journal of Cleaner Production, 2017. **166**: p. 1043-1058.

71. Mohd, N.H., et al., *Effect of aminosilane modification on nanocrystalline cellulose properties*. Journal of Nanomaterials, 2016. **2016**.

72. Zarshenas, K., A. Raisi, and A. Aroujalian, *Mixed matrix membrane of nano-zeolite NaX/poly (ether-block-amide) for gas separation applications*. Journal of Membrane Science, 2016. **510**: p. 270-283.

73. Li, M., et al., *Pebax-based composite membranes with high gas transport properties enhanced by ionic liquids for CO 2 separation*. RSC Advances, 2017. **7**(11): p. 6422-6431.

74. Ghadimi, A., et al., *Preparation of alloyed poly (ether block amide)/poly (ethylene glycol diacrylate) membranes for separation of $CO_2/H_2$ (syngas application)*. Journal of membrane science, 2014. **458**: p. 14-26.

75.     Jusoh, N., et al., *Enhanced gas separation performance using mixed matrix membranes containing zeolite T and 6FDA-durene polyimide.* Journal of membrane science, 2017. **525**: p. 175-186.

76.     Habibiannejad, S., A. Aroujalian, and A. Raisi, *Pebax-1657 mixed matrix membrane containing surface modified multi-walled carbon nanotubes for gas separation.* RSC Advances, 2016. **6**(83): p. 79563-79577.

# VITA

**NAME**              Thakorn Wichaidit

**DATE OF BIRTH**     7 Oct 1993

**PLACE OF BIRTH**    Bangkok

**INSTITUTIONS**      Bachelor of Engineering Program in Chemical
**ATTENDED**          Engineering
**HOME ADDRESS**      49/1248,  Moo 2, Chaengwattana Rd., Bangtalad sub-
                      district, Pakkret district, Nonthaburi, 11120, Thailand
**PUBLICATION**       The 6th Thailand International Nanotechnology
                      Conference (NanoThailand 2018): Composite hollow fiber
                      membrane of modified zeolite Y for biogas upgrading

จุฬาลงกรณ์มหาวิทยาลัย

CHULALONGKORN UNIVERSITY